Hindawi
International Journal of Photoenergy
Volume 2017, Article ID 2532109, 19 pages
https://doi.org/10.1155/2017/2532109

Research Article

An Improved Generalized Method for Evaluation of Parameters, Modeling, and Simulation of Photovoltaic Modules

Vandana Jha and Uday Shankar Triar

Electrical Engineering Department, National Institute of Technology Patna, Bihar, India

Correspondence should be addressed to Vandana Jha; vandanajha.electrical@gmail.com

Received 12 July 2017; Accepted 25 September 2017; Published 3 December 2017

Academic Editor: Francesco Riganti Fulginei

This paper proposes an improved generalized method for evaluation of parameters, modeling, and simulation of photovoltaic modules. A new concept "Level of Improvement" has been proposed for evaluating unknown parameters of the nonlinear *I-V* equation of the single-diode model of PV module at any environmental condition, taking the manufacturer-specified data at Standard Test Conditions as inputs. The main contribution of the new concept is the improvement in the accuracy of values of evaluated parameters up to various levels and is based on mathematical equations of PV modules. The proposed evaluating method is implemented by MATLAB programming and, for demonstration, by using the values of parameters of the *I-V* equation obtained from programming results, a PV module model is build with MATLAB. The parameters evaluated by the proposed technique are validated with the datasheet values of six different commercially available PV modules (thin film, monocrystalline, and polycrystalline) at Standard Test Conditions and Nominal Operating Cell Temperature Conditions. The module output characteristics generated by the proposed method are validated with experimental data of FS-270 PV module. The effects of variation of ideality factor and resistances on output characteristics are also studied. The superiority of the proposed technique is proved.

1. Introduction

Photovoltaics (PV) is a method of converting sunlight directly into electricity using semiconducting materials that exhibit the photovoltaic effect. A PV cell is the fundamental PV device. A PV cell is a specialized semiconductor diode that converts sunlight into direct current (DC) electricity. A PV module is a collection of PV cells wired in series/parallel combinations as required to meet current and voltage requirements. A PV panel includes one or more PV modules assembled as a prewired, field-installable unit. A PV array is the complete power-generating unit, consisting of any number of PV panels to form large PV systems.

PV cells are expensive, and the characteristics of PV devices are highly dependent on environmental conditions [1]. Therefore, to ensure the maximum use of the available solar energy by a PV power system, it is important to study its behaviour through modeling, before implementing it in reality. The mathematical model of the PV device is very useful in studying various PV technologies and in designing several PV systems along with their components for application in practical systems.

The equivalent circuit of the ideal PV cell is represented basically by (i) single-diode model [1–7] and (ii) two-diode model [8–12]. In single-diode model, the effect of the recombination loss of carriers in the depletion region is not considered, whereas in two-diode model, an additional diode is included to consider this effect. Many more sophisticated models have been developed so far to include the effects that are not considered by the earlier models, thus claiming more accuracy. The single-diode model is simple and accurate and is perfect for designers who are looking for a model for the modeling of PV devices where the intended result is achieved without great effort [4, 13].

The parameter identification of the single-diode model with five parameters has been enormously researched [1–7]. The information provided in the datasheet cannot saturate the necessary restrictions to calculate the five unknown parameters. Consequently, some presumptions and approximations are generally needed to initiate the parameter extraction. For example, in [4], the evaluation of both photovoltaic current (I_{pv}) and diode reverse saturation current (I_0) is based on approximation, due to which the deviation at open and short conditions becomes inevitable, and the diode ideality constant (a) has been assumed on the basis of PV cell technology. Since this constant affects the curvature of the I-V curves and its correct estimation improves the model accuracy, it must be evaluated accurately without assumption. A separate DC circuit is constructed to determine ideality constant in [1], thus increasing the cost of the evaluation procedure. Some other techniques adopted by the authors to estimate the ideality constant are curve fitting [6, 14], iteration [7], trial and error [14], and the concept of the minimum sum of squares [15]. But for evaluating ideality constant by any of the above methods, manufacturer-specified output characteristics are required. Thus, these processes can be cumbersome. Also, in some PV module datasheets, output characteristics are not given [16]. Therefore, evaluating ideality constant of such modules becomes very difficult.

Apart from the evaluation of I_{pv}, I_0, and a, extensive studies have been conducted to determine the series resistance (R_s) and parallel resistance (R_p). Some authors neglect R_p to simplify the model as the value of this resistance is generally high [14–19], and sometimes, the R_s is neglected, as its value is very low [20, 21]. The neglect of R_s and R_p has significant impact on the model accuracy. Several algorithms have been proposed to determine both R_s and R_p through iterative techniques [4, 12]. If the initialisation of the variables and the convergence conditions are not proper, then these iterative techniques require many iterations and, sometimes, may not converge. Curve fitting method can be utilized in the current density-voltage curves to estimate both R_s and R_p [22]. In [23], R_s and R_p are evaluated by using additional parameters which can be extracted from the current versus voltage curve of a PV module. These methods are quite poor, inaccurate, and tedious mainly because R_s and R_p are adjusted separately, which is not a good practice, if an accurate model is required. Moreover, these methods are applicable only if the manufacturer-specified output characteristics are provided. Differential evolution (DE) can be used to extract the excess seven parameters of a double-diode PV module model utilising only the information provided in the datasheets [8, 10]. An explicit modeling method based on Lambert W-function for PV arrays that has been used in [24] to find the values of parameters is intricate and time-consuming. Artificial intelligence (AI) such as fuzzy logic [25] and artificial neural network (ANN) [26, 27] and genetic algorithms such as particle swarm optimization (PSO) have also been proposed to model the I-V curves [28]. However, they are not widely adopted due to high computation burden. In [2], a comprehensive parameter identification method is proposed to enhance model accuracy while keeping the parameterization procedure in a simple form. Despite the accurate results, the approach requires extensive computation. A circuit-based piecewise linear PV device model has been developed and demonstrated using PSCAD/EMTDC for parameter identification [29]. As this method is based on trial and error for different values of irradiance and temperature and is based on a large number of approximations and assumptions, this method becomes complicated and less accurate.

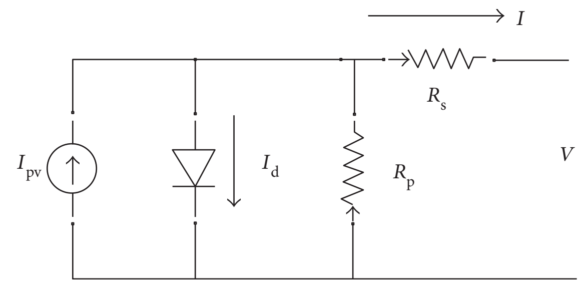

Figure 1: Single-diode equivalent circuit of a practical PV module.

Hence, to overcome the above drawbacks, an improved generalized method for evaluation of parameters, modeling, and simulation of photovoltaic modules has been proposed in this paper. A new concept "Level of Improvement" has been proposed for evaluating unknown parameters of the nonlinear I-V equation of the single-diode model of PV module including series and parallel resistances at any environmental condition (STC and NOCTC in this paper), taking the manufacturer-specified data at Standard Test Conditions as inputs. The new concept helps in improving the accuracy of the values of evaluated parameters up to various levels. The proposed evaluating method is based on mathematical equations of PV modules, thus making the method fast, simple, and accurate. The method for evaluating a is based on the property that at the maximum power point, $dP/dV = 0$. The proposed evaluating method is implemented by MATLAB programming and by using the values of parameters of the I-V equation obtained from programming results, a PV module model is build with MATLAB. The parameters evaluated by the proposed technique are validated with the datasheet values of six different commercially available PV modules for irradiance and temperature at Standard Test Conditions and Nominal Operating Cell Temperature Conditions. The module output characteristics generated by the proposed method are validated with experimental data of FS-270 PV module at different environmental conditions (varying irradiance and temperature). The effects of variation of ideality factor and resistances on the output characteristics are also studied. The superiority of the proposed technique over three popular existing techniques [4, 6, 12] is proved.

2. Mathematical Equation and Modeling of Photovoltaic Modules

Practical modules are composed of various PV cells connected in series or parallel. Figure 1 shows the single-diode equivalent circuit of a practical PV module.

The mathematical equation that describes the I-V characteristic of a practical PV module is

$$I = I_{pv} - I_0\left[\exp\left(\frac{V + R_s I}{V_t a}\right) - 1\right] - \frac{V + R_s I}{R_p}, \quad (1)$$

$$I = I_{pv,cell}N_p - I_{0,cell}N_p\left[\exp\left(\frac{V + R_s I}{V_t a}\right) - 1\right] - \frac{V + R_s I}{R_p}, \quad (2)$$

$$V_t = \frac{N_s kT}{q}. \quad (3)$$

The equation that mathematically describes the *P-V* characteristic of a practical PV module is

$$P = V\left[I_{pv} - I_0\left\{\exp\left(\frac{V + R_s I}{V_t a}\right) - 1\right\} - \frac{V + R_s I}{R_p}\right]. \quad (4)$$

For the observation of the characteristics of the PV module, it is required to evaluate all the parameters of (1) [6]. Datasheets generally give information about the parameters, characteristics, and performances of PV modules with respect to the Standard Test Condition (STC), which is taken as 1000 W/m^2 solar irradiance and 25°C module temperature [30–36]. Some datasheets also give information about PV modules at Nominal Operating Cell Temperature Condition (NOCTC), which is generally taken as 800 W/m^2 irradiance and 20°C ambient temperature. The parameters basically present in all PV module datasheets at STC and sometimes at NOCTC are as follows: P_{mpp}, V_{mpp}, I_{mpp}, V_{oc}, I_{sc}, $K^T_{P_{mpp}}$, $K^T_{V_{mpp}}$, $K^T_{I_{mpp}}$, $K^T_{V_{oc}}$, and $K^T_{I_{sc}}$ for any environmental condition. Table 1 shows the values of the parameters of seven different commercially available photovoltaic modules at STC provided by the manufacturers [30–36].

Some of the parameters of (4) can be found in the manufacturer's datasheets. The remaining parameters such as I_{pv}, a, I_0, R_s, and R_p have to be evaluated. They are usually not specified by the manufacturers because they cannot be measured and are unique for every module [19].

3. Basic Evaluation of the Parameters

The proposed work attempts to evaluate the five unknown parameters (I_{pv}, a, I_0, R_s, and R_p) of a PV module at different environmental conditions.

3.1. Evaluation of Photovoltaic Current. The parallel resistance R_p is generally very high, so the last term of (1) can be eliminated for the further work.

$$I = I_{pv} - I_0\left[\exp\left(\frac{V + R_s I}{V_t a}\right) - 1\right]. \quad (5)$$

By applying short-circuit condition ($I = I_{sc}$, $V = 0$) to (5), (6) can be derived as follows:

$$I_{sc} = I_{pv} - I_0\left[\exp\left(\frac{I_{sc} R_s}{V_t a}\right) - 1\right]. \quad (6)$$

Since ($I_0[\exp(I_{sc}R_s/V_t a) - 1] \approx 0$), (6) can be written as

$$I_{pv} \approx I_{sc}. \quad (7)$$

The photovoltaic current of a PV module is approximately equal to the short-circuit current at any environmental condition.

3.2. Evaluation of Diode Ideality Constant. By applying open-circuit condition ($I = 0$, $V = V_{oc}$) to (5), (8) can be derived as follows:

$$0 = I_{pv} - I_0\left[\exp\left(\frac{V_{oc}}{V_t a}\right) - 1\right]. \quad (8)$$

By rearranging (8), (9) is obtained as follows:

$$I_0 = \frac{I_{pv}}{[\exp(V_{oc}/V_t a) - 1]}. \quad (9)$$

In the proposed method, the maximum power point is considered for evaluating "a" using the property $dP/dV = 0$ at the maximum power point.

$$P = VI, \quad (10)$$

$$\frac{1}{V}\cdot\frac{dP}{dV} = \frac{dI}{dV} + \frac{I}{V}. \quad (11)$$

By applying maximum power condition to (11), (12) is obtained as follows:

$$\left.\frac{dI}{dV}\right|_{mpp} + \frac{I_{mpp}}{V_{mpp}} = 0. \quad (12)$$

By differentiating (5) and applying maximum power condition, (13) can be obtained as follows:

$$\left.\frac{dI}{dV}\right|_{mpp} = \frac{(-I_0/V_t)\exp\left(\left(V_{mpp} + I_{mpp}R_s\right)/V_t a\right)}{a + (I_0/V_t)R_s\exp\left(\left(V_{mpp} + I_{mpp}R_s\right)/V_t a\right)}. \quad (13)$$

By substituting (13) in (12), (14) can be obtained as follows:

$$\frac{aI_{mpp} + \left(I_{mpp}R_s - V_{mpp}\right)(I_0/V_t)\exp\left(\left(V_{mpp} + I_{mpp}R_s\right)/V_t a\right)}{\left[a + (I_0/V_t)R_s\exp\left(\left(V_{mpp} + I_{mpp}R_s\right)/V_t a\right)\right]V_{mpp}} = 0. \quad (14)$$

For (14) to be valid, the numerator of (14) must be zero as the denominator is finite.

$$aI_{mpp} + \left(I_{mpp}R_s - V_{mpp}\right)\frac{I_0}{V_t}\exp\left(\frac{V_{mpp} + I_{mpp}R_s}{V_t a}\right) = 0. \quad (15)$$

By applying maximum power point condition to (5) and rearranging terms, (16) and (17) can be obtained as follows:

$$\exp\left(\frac{V_{mpp} + I_{mpp}R_s}{V_t a}\right) = \frac{I_{pv} - I_{mpp} + I_0}{I_0}, \quad (16)$$

$$R_s = \frac{V_t a}{I_{mpp}}\ln\left(\frac{I_{pv} - I_{mpp} + I_0}{I_0}\right) - \frac{V_{mpp}}{I_{mpp}}. \quad (17)$$

Table 1: Parameters of seven different commercially available PV modules at STC (25°C and 1000 W/m^2) provided by the manufacturers [30–36].

Parameter	Thin film		Monocrystalline		Multicrystalline		
	Shell ST40	FS-270	Shell SQ 150-PC	HIT-N240SE10	KD140GX-LFBS	KD260GX-LFB2	KU265-6MCA
$P_{\mathrm{mpp_{STC}}}$ W	40	70	150	240	140	260	265
$V_{\mathrm{mpp_{STC}}}$ V	16.6	65.5	34	43.7	17.7	31.0	31.0
$I_{\mathrm{mpp_{STC}}}$ A	2.41	1.07	4.4	5.51	7.91	8.39	8.55
$V_{\mathrm{oc_{STC}}}$ V	23.3	88.0	43.4	52.4	22.1	38.3	38.3
$I_{\mathrm{sc_{STC}}}$ A	2.68	1.23	4.8	5.85	8.68	9.09	9.26
$K^T_{P_{\mathrm{mpp}}}$	−0.6%/°C	−0.25%/°C	−0.52%/°C	−0.30%/°C	−0.46%/°C	−0.45%/°C	−0.45%/°C
$K^T_{V_{\mathrm{mpp}}}$	−100 mV/°C	−0.34%/°C	−167 mV/°C	−0.131 V/°C	−0.52%/°C	−0.48%/°C	−0.48%/°C
$K^T_{I_{\mathrm{mpp}}}$	−2.50 mA/°C	0.023%/°C	−2.38 mA/°C	2.105 mA/°C	0.0066%/°C	0.02%/°C	0.02%/°C
$K^T_{V_{\mathrm{oc}}}$	−100 mV/°C	−0.25%/°C	−161 mV/°C	−0.131 V/°C	−0.36%/°C	−0.36%/°C	−0.36%/°C
$K^T_{I_{\mathrm{sc}}}$	0.35 mA/°C	0.04%/°C	1.4 mA/°C	1.76 mA/°C	0.060%/°C	0.06%/°C	0.06%/°C
N_{s}	36	116	72	72	36	60	60
N_{p}	1	1	1	1	1	1	1

By combining (16) and (17), (18) can be obtained as follows:

$$aI_{\mathrm{mpp}} + \left(I_{\mathrm{pv}} - I_{\mathrm{mpp}} + I_0\right) \cdot \left\{ a \ln\left(\frac{I_{\mathrm{pv}} - I_{\mathrm{mpp}} + I_0}{I_0}\right) - \frac{2V_{\mathrm{mpp}}}{V_{\mathrm{t}}} \right\} = 0. \tag{18}$$

Substituting (7) and (9) in (18), (19) is obtained as follows:

$$aI_{\mathrm{mpp}} + \left(I_{\mathrm{sc}} - I_{\mathrm{mpp}} + \frac{I_{\mathrm{sc}}}{[\exp(V_{\mathrm{oc}}/V_{\mathrm{t}}a) - 1]}\right) \cdot \left\{ a \ln\left(\frac{I_{\mathrm{sc}} - I_{\mathrm{mpp}} + (I_{\mathrm{sc}}/[\exp(V_{\mathrm{oc}}/V_{\mathrm{t}}a) - 1])}{I_{\mathrm{sc}}/[\exp(V_{\mathrm{oc}}/V_{\mathrm{t}}a) - 1]}\right) - \frac{2V_{\mathrm{mpp}}}{V_{\mathrm{t}}} \right\} = 0. \tag{19}$$

When the data specified in the manufacturer's datasheets are used, the left hand side of (19) becomes a function of "a" and it is denoted by $f(a)$.

$$f(a) = aI_{\mathrm{mpp}} + \left(I_{\mathrm{sc}} - I_{\mathrm{mpp}} + \frac{I_{\mathrm{sc}}}{[\exp(V_{\mathrm{oc}}/V_{\mathrm{t}}a) - 1]}\right) \cdot \left\{ a \ln\left(\frac{I_{\mathrm{sc}} - I_{\mathrm{mpp}} + (I_{\mathrm{sc}}/[\exp(V_{\mathrm{oc}}/V_{\mathrm{t}}a) - 1])}{I_{\mathrm{sc}}/[\exp(V_{\mathrm{oc}}/V_{\mathrm{t}}a) - 1]}\right) - \frac{2V_{\mathrm{mpp}}}{V_{\mathrm{t}}} \right\}. \tag{20}$$

Thus, "a" is found by solving $f(a) = 0$ with the help of MATLAB programming.

3.3. Evaluation of Diode Reverse Saturation Current. By (9), the diode reverse saturation current at any environmental condition can be obtained.

3.4. Evaluation of Series and Parallel Resistances. Equating the maximum power calculated by the P-V model of (4) ($P_{\mathrm{mpp\,cal}}$) to the power at the MPP from the datasheet (P_{mpp}) at any environmental condition, a relation between R_{s} and R_{p} will be obtained, that is,

$$P_{\mathrm{mpp\,cal}} = P_{\mathrm{mpp}}, \tag{21}$$

$$P_{\mathrm{mpp\,cal}} = V_{\mathrm{mpp}} I_{\mathrm{mpp}} = V_{\mathrm{mpp}} \left\{ I_{\mathrm{pv}} - I_0 \left[\exp\left(\frac{V_{\mathrm{mpp}} + R_{\mathrm{s}} I_{\mathrm{mpp}}}{V_{\mathrm{t}} a}\right) - 1 \right] - \frac{V_{\mathrm{mpp}} + R_{\mathrm{s}} I_{\mathrm{mpp}}}{R_{\mathrm{p}}} \right\} = P_{\mathrm{mpp}}, \tag{22}$$

$$R_{\mathrm{p}} = \frac{V_{\mathrm{mpp}}\left(V_{\mathrm{mpp}} + I_{\mathrm{mpp}} R_{\mathrm{s}}\right)}{V_{\mathrm{mpp}} I_{\mathrm{pv}} - V_{\mathrm{mpp}} I_0 \exp\left[\left(V_{\mathrm{mpp}} + I_{\mathrm{mpp}} R_{\mathrm{s}}\right)/V_{\mathrm{t}} a\right] + V_{\mathrm{mpp}} I_0 - P_{\mathrm{mpp}}}. \tag{23}$$

According to (23), for any value of R_{s}, there will be a value of R_{p} that satisfies (21). It is required to find an only pair of R_{s} and R_{p} for the desired environmental condition that satisfies the model accurately.

3.4.1. Proposed Algorithm. In this work, R_{s} and R_{p} in (23) are calculated through the following steps:

(a) Eliminating the last term of (4), as the value of the parallel resistance is high, the power calculated by the P-V model excluding R_{p}, $P_{\mathrm{without}\,R_{\mathrm{p}}}$ is obtained as follows:

$$P_{\mathrm{without}\,R_{\mathrm{p}}} = V \left\{ I_{\mathrm{pv}} - I_0 \left[\exp\left(\frac{V + R_{\mathrm{smax}'} I_{\mathrm{without}\,R_{\mathrm{p}}}}{V_{\mathrm{t}} a}\right) - 1 \right] \right\}. \tag{24}$$

(b) Iterations are performed on (24) where $R_{\mathrm{smax}'}$ is slowly incremented starting from $R_{\mathrm{smax}'} = 0$, till the maximum of power calculated by the P-V model excluding R_p $(\max(P_{\text{without } R_p}))$ becomes approximately equal to the power at the MPP from the datasheet (P_{mpp}).

(c) Putting $R_s = R_{smax}$ in (23), the value of R_p obtained is negative. Iterations are performed again on (23), where R_s is slowly decremented starting from $R_s = R_{smax}$, until a positive value for R_p is obtained. Hence, the maximum value of parallel resistance R_{pmax} is obtained and the corresponding value of series resistance is the maximum value of series resistance, R_{smax}.

(d) Putting $R_s = 0$ in (23), the minimum value of parallel resistance R_{pmin} is obtained as follows:

$$R_{pmin} = \frac{V_{mpp}}{I_{pv} - I_0 \exp\left[V_{mpp}/V_t a\right] + I_0 - \left(P_{mpp}/V_{mpp}\right)}. \quad (25)$$

The value of R_{pmin} obtained by the proposed method is more accurate as compared to other methods [4, 12].

(e) Initialising $R_s = R_{smax}$ and $R_p = R_{pmax}$, iterations are performed again on (4) where R_s is slowly decremented and the corresponding value of R_p is obtained, till the maximum of power calculated by the P-V model $(\max(P))$ becomes approximately equal to the power at the MPP from the datasheet (P_{mpp}), while $R_p > R_{pmin}$. Thus, R_s and R_p are obtained.

4. Improving the Model

The accuracy of the values of evaluated parameters (I_{pv}, a, I_0, R_s, and R_p) is improved up to various levels by using "Level of Improvement."

4.1. First Level of Improvement

4.1.1. Evaluation of Photovoltaic Current. By applying short-circuit condition ($I = I_{sc}$, $V = 0$) to (5), (26) can be derived as follows:

$$I_{sc} = I_{pv}1 - I_0 1\left[\exp\left(\frac{I_{sc}R_s}{V_t a1}\right) - 1\right] - \frac{R_s I_{sc}}{R_p}. \quad (26)$$

Since $(I_0 1[\exp(I_{sc}R_s/V_t a1) - 1] \approx 0)$, (26) can be written as

$$I_{pv}1 \approx I_{sc}\left(1 + \frac{R_s}{R_p}\right). \quad (27)$$

By (27), the first level of improved value of photovoltaic current of a PV module ($I_{pv}1$) at any environmental condition can be obtained.

4.1.2. Evaluation of Diode Ideality Constant. By applying open-circuit condition ($I = 0$, $V = V_{oc}$) to (5), (28) can be derived as follows:

$$0 = I_{pv}1 - I_0 1\left[\exp\left(\frac{V_{oc}}{V_t a1}\right) - 1\right] - \frac{V_{oc}}{R_p}. \quad (28)$$

By rearranging (28), (29) is obtained as follows:

$$I_0 1 = \frac{I_{pv}1 - \left(V_{oc}/R_p\right)}{\left[\exp(V_{oc}/V_t a1) - 1\right]}. \quad (29)$$

By applying the same procedure as is applied on (5) to find the diode ideality constant on (1), an improved and more accurate value of diode ideality constant can be obtained, as the values of both R_s and R_p are taken into account.

The function $f(a1)$, where $a1$ is the first level of improved value of diode ideality constant, becomes

$$\begin{aligned} f(a1) = {} & \left\{ R_p \left(I_{sc}\left(1 + \frac{R_s}{R_p}\right) - I_{mpp} \right.\right. \\ & \left. + \frac{I_{sc}\left(1 + \left(R_s/R_p\right)\right) - \left(V_{oc}/R_p\right)}{\left[\exp(V_{oc}/V_t a1) - 1\right]} \right) \\ & \left. - \left(V_{mpp} + R_s I_{mpp}\right) \right\} \left(-V_{mpp} + R_s I_{mpp}\right) \\ & - V_t a1 \left(V_{mpp} - R_p I_{mpp} - R_s I_{mpp}\right). \end{aligned} \quad (30)$$

Thus, "$a1$" is found by solving $f(a1) = 0$ with the help of MATLAB programming.

4.1.3. Evaluation of Diode Reverse Saturation Current. By (29), the first level of improved value of diode reverse saturation current ($I_0 1$) at any environmental condition can be obtained.

4.1.4. Evaluation of Series and Parallel Resistances. By applying the same procedure as is applied to evaluate R_s and R_p, a first level of improved values of series resistance ($R_s 1$) and parallel resistance ($R_p 1$) for the desired environmental condition can be found.

4.2. Second Level of Improvement. Again by putting $R_s = R_s 1$ and $R_p = R_p 1$ in (27) and (30), a second level of improved value of photovoltaic current ($I_{pv}2$) and diode ideality constant ($a2$) can be obtained. As a consequence, a second level of improved value of diode reverse saturation current ($I_0 2$), series resistance ($R_s 2$), and parallel resistance ($R_p 2$) can be obtained. The improvement can go up to ith level ($I_{pv}i$, ai, $I_0 i$, $R_s i$, and $R_p i$), till the errors between the values of parameters evaluated by the proposed method and the values of parameters provided in manufacturer's datasheet become minimum.

It should also be noted that the value of diode ideality constant should not vary much in any level of improvement. This is possible only when the value of parallel resistance is high. In the proposed method, initialising the series and parallel resistances by their corresponding maximum values in

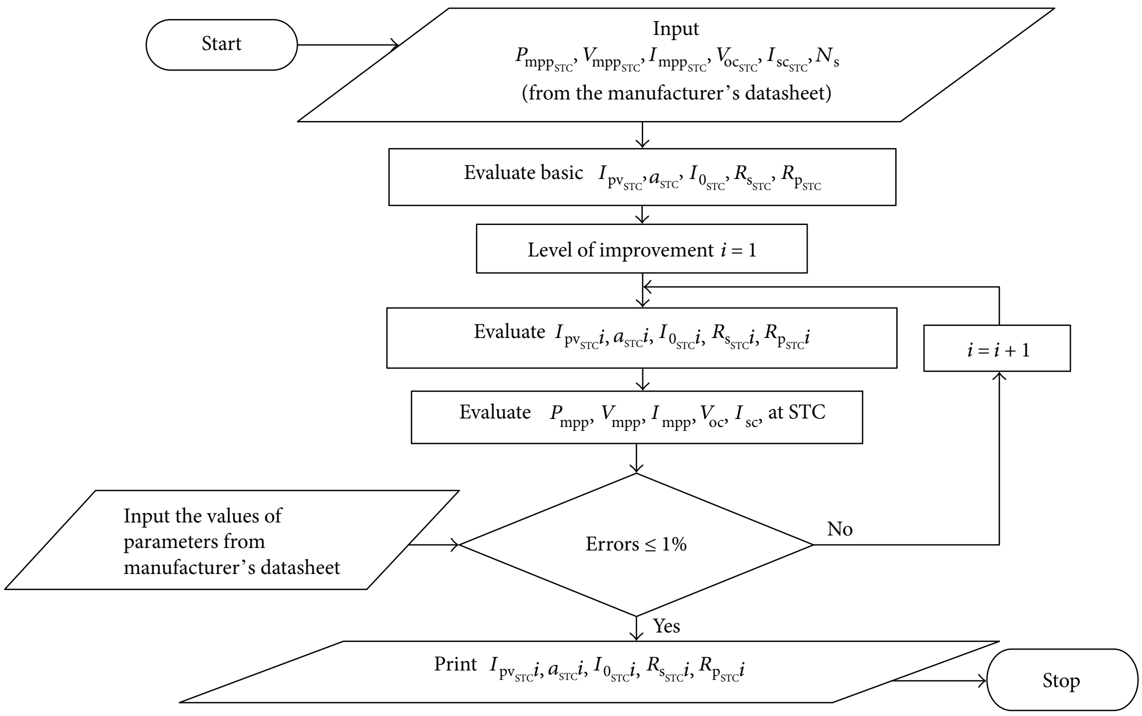

Figure 2: Flowchart for evaluation of five unknown parameters ($I_{\text{pv}_{\text{STC}}}$, a_{STC}, $I_{0_{\text{STC}}}$, $R_{\text{s}_{\text{STC}}}$, and $R_{\text{p}_{\text{STC}}}$) of a PV module at STC.

every level of improvement helps in getting higher value of parallel resistance and also reduces the required number of iterations. In this paper, only the first level of improvement has been applied.

5. Dependence of Parameters of the Characteristic Equation of the PV Module on Irradiance and Temperature

The V_{oc}, I_{sc}, V_{mpp}, I_{mpp}, and P_{mpp} of the PV module depend on both solar irradiance and temperature and can be calculated using the following equations:

$$V_{\text{oc}} = \left(1 + K^{G}_{V_{\text{oc}}}\left(\log\left(\frac{G}{G_{\text{STC}}}\right)\right)\right)\left(V_{\text{oc}_{\text{STC}}} + K^{T}_{V_{\text{oc}}}\Delta T\right), \tag{31}$$

$$I_{\text{sc}} = \frac{G}{G_{\text{STC}}}\left(I_{\text{sc}_{\text{STC}}} + K^{T}_{I_{\text{sc}}}\Delta T\right), \tag{32}$$

$$V_{\text{mpp}} = \left(1 + K^{G}_{V_{\text{mpp}}}\left(\log\left(\frac{G}{G_{\text{STC}}}\right)\right)\right)\left(V_{\text{mpp}_{\text{STC}}} + K^{T}_{V_{\text{mpp}}}\Delta T\right), \tag{33}$$

$$I_{\text{mpp}} = \frac{G}{G_{\text{STC}}}\left(I_{\text{mpp}_{\text{STC}}} + K^{T}_{I_{\text{mpp}}}\Delta T\right), \tag{34}$$

$$P_{\text{mpp}} = \frac{G}{G_{\text{STC}}}\left(1 + K^{G}_{P_{\text{mpp}}}\left(\log\left(\frac{G}{G_{\text{STC}}}\right)\right)\right) \cdot \left(P_{\text{mpp}_{\text{STC}}} + K^{T}_{P_{\text{mpp}}}\Delta T\right), \tag{35}$$

$$\Delta T = T - T_{\text{STC}}. \tag{36}$$

6. Evaluation of Parameters of the Characteristic Equation of the PV Module at STC

Applying STC to the above procedure and using the manufacturer-specified data at Standard Test Condition, five unknown parameters ($I_{\text{pv}_{\text{STC}}}$, a_{STC}, $I_{0_{\text{STC}}}$, $R_{\text{s}_{\text{STC}}}$, and $R_{\text{p}_{\text{STC}}}$) of a PV module at STC can be evaluated.

The flowchart for evaluation of five unknown parameters ($I_{\text{pv}_{\text{STC}}}$, a_{STC}, $I_{0_{\text{STC}}}$, $R_{\text{s}_{\text{STC}}}$, and $R_{\text{p}_{\text{STC}}}$) of a PV module at STC is presented in Figure 2.

Table 2 shows the first level of improved values of the parameters of seven different commercially available PV modules for the proposed model and evaluated parameters of seven different commercially available PV modules for the R_s model [6], R_s and R_p model [4], and two-diode model [12] at STC.

7. Evaluation of Parameters of the Characteristic Equation of the PV Module at NOCTC

Using the manufacturer-specified data at STC and NOCTC in (31), (33), and (35) irradiance coefficients of V_{oc}, V_{mpp}, and P_{mpp} of the PV module can be calculated.

Five unknown parameters of a PV module at NOCTC can be evaluated using the following equations:

$$
\begin{aligned}
I_{\mathrm{pv}_{\mathrm{NOCTC}}}1 &\approx \Bigl(\frac{G_{\mathrm{NOCTC}}}{G_{\mathrm{STC}}}\Bigl(I_{\mathrm{sc}_{\mathrm{STC}}} + K_{I_{\mathrm{sc}}}^{T}\Delta T\Bigr)\Bigr)\Bigl(1 + \frac{R_{\mathrm{s}_{\mathrm{NOCTC}}}}{R_{\mathrm{p}_{\mathrm{NOCTC}}}}\Bigr),\\
f(a_{\mathrm{NOCTC}}1) &= \Bigl\{R_{\mathrm{p}_{\mathrm{NOCTC}}}\Bigl(\Bigl(\frac{G_{\mathrm{NOCTC}}}{G_{\mathrm{STC}}}\Bigl(I_{\mathrm{sc}_{\mathrm{STC}}} + K_{I_{\mathrm{sc}}}^{T}\Delta T\Bigr)\Bigr)\Bigl(1 + \frac{R_{\mathrm{s}_{\mathrm{NOCTC}}}}{R_{\mathrm{p}_{\mathrm{NOCTC}}}}\Bigr) - \Bigl(\frac{G_{\mathrm{NOCTC}}}{G_{\mathrm{STC}}}\Bigl(I_{\mathrm{mpp}_{\mathrm{STC}}} + K_{I_{\mathrm{mpp}}}^{T}\Delta T\Bigr)\Bigr)\\
&\quad + \frac{\Bigl((G_{\mathrm{NOCTC}}/G_{\mathrm{STC}})\Bigl(I_{\mathrm{sc}_{\mathrm{STC}}} + K_{I_{\mathrm{sc}}}^{T}\Delta T\Bigr)\Bigr)\Bigl(\Bigl(1 + \Bigl(R_{\mathrm{s}_{\mathrm{NOCTC}}}/R_{\mathrm{p}_{\mathrm{NOCTC}}}\Bigr)\Bigr) - \Bigl(\Bigl(1 + K_{V_{\mathrm{oc}}}^{G}(\log(G_{\mathrm{NOCTC}}/G_{\mathrm{STC}}))\Bigr)\Bigl(V_{\mathrm{oc}_{\mathrm{STC}}} + K_{V_{\mathrm{oc}}}^{T}\Delta T\Bigr)\Bigr)/R_{\mathrm{p}_{\mathrm{NOCTC}}}\Bigr)}{\Bigl[\exp\Bigl(\Bigl(\Bigl(1 + K_{V_{\mathrm{oc}}}^{G}(\log(G_{\mathrm{NOCTC}}/G_{\mathrm{STC}}))\Bigr)\Bigl(V_{\mathrm{oc}_{\mathrm{STC}}} + K_{V_{\mathrm{oc}}}^{T}\Delta T\Bigr)\Bigr)/V_{\mathrm{t}_{\mathrm{NOCTC}}}a_{\mathrm{NOCTC}}1\Bigr) - 1\Bigr]}\Bigr)\\
&\quad - \Bigl(\Bigl(\Bigl(1 + K_{V_{\mathrm{mpp}}}^{G}\Bigl(\log\Bigl(\frac{G_{\mathrm{NOCTC}}}{G_{\mathrm{STC}}}\Bigr)\Bigr)\Bigr)\Bigl(V_{\mathrm{mpp}_{\mathrm{STC}}} + K_{V_{\mathrm{mpp}}}^{T}\Delta T\Bigr)\Bigr) + R_{\mathrm{s}_{\mathrm{NOCTC}}}\Bigl(\frac{G_{\mathrm{NOCTC}}}{G_{\mathrm{STC}}}\Bigl(I_{\mathrm{mpp}_{\mathrm{STC}}} + K_{I_{\mathrm{mpp}}}^{T}\Delta T\Bigr)\Bigr)\Bigr)\Bigr\}\\
&\quad \cdot \Bigl(-\Bigl(\Bigl(1 + K_{V_{\mathrm{mpp}}}^{G}\Bigl(\log\Bigl(\frac{G_{\mathrm{NOCTC}}}{G_{\mathrm{STC}}}\Bigr)\Bigr)\Bigr)\Bigl(V_{\mathrm{mpp}_{\mathrm{STC}}} + K_{V_{\mathrm{mpp}}}^{T}\Delta T\Bigr)\Bigr) + R_{\mathrm{s}_{\mathrm{NOCTC}}}\Bigl(\frac{G_{\mathrm{NOCTC}}}{G_{\mathrm{STC}}}\Bigl(I_{\mathrm{mpp}_{\mathrm{STC}}} + K_{I_{\mathrm{mpp}}}^{T}\Delta T\Bigr)\Bigr)\Bigr)\\
&\quad - V_{\mathrm{t}_{\mathrm{NOCTC}}}a_{\mathrm{NOCTC}}1\Bigl(\Bigl(\Bigl(1 + K_{V_{\mathrm{mpp}}}^{G}(\log(G_{\mathrm{NOCTC}}/G_{\mathrm{STC}}))\Bigr)\Bigl(V_{\mathrm{mpp}_{\mathrm{STC}}} + K_{V_{\mathrm{mpp}}}^{T}\Delta T\Bigr)\Bigr)\\
&\quad - R_{\mathrm{p}_{\mathrm{NOCTC}}}\Bigl(\frac{G_{\mathrm{NOCTC}}}{G_{\mathrm{STC}}}\Bigl(I_{\mathrm{mpp}_{\mathrm{STC}}} + K_{I_{\mathrm{mpp}}}^{T}\Delta T\Bigr)\Bigr) - R_{\mathrm{s}_{\mathrm{NOCTC}}}\Bigl(\frac{G_{\mathrm{NOCTC}}}{G_{\mathrm{STC}}}\Bigl(I_{\mathrm{mpp}_{\mathrm{STC}}} + K_{I_{\mathrm{mpp}}}^{T}\Delta T\Bigr)\Bigr)\Bigr),\\
I_{0_{\mathrm{NOCTC}}}1 &= \frac{\Bigl(\Bigl((G_{\mathrm{NOCTC}}/G_{\mathrm{STC}})\Bigl(I_{\mathrm{sc}_{\mathrm{STC}}} + K_{I_{\mathrm{sc}}}^{T}\Delta T\Bigr)\Bigr)\Bigl(1 + \Bigl(R_{\mathrm{s}_{\mathrm{NOCTC}}}/R_{\mathrm{p}_{\mathrm{NOCTC}}}\Bigr)\Bigr)\Bigr) - \Bigl(\Bigl(\Bigl(1 + K_{V_{\mathrm{oc}}}^{G}(\log(G_{\mathrm{NOCTC}}/G_{\mathrm{STC}}))\Bigr)\Bigl(V_{\mathrm{oc}_{\mathrm{STC}}} + K_{V_{\mathrm{oc}}}^{T}\Delta T\Bigr)\Bigr)/R_{\mathrm{p}_{\mathrm{NOCTC}}}\Bigr)}{\Bigl[\exp\Bigl(\Bigl(\Bigl(1 + K_{V_{\mathrm{oc}}}^{G}(\log(G_{\mathrm{NOCTC}}/G_{\mathrm{STC}}))\Bigr)\Bigl(V_{\mathrm{oc}_{\mathrm{STC}}} + K_{V_{\mathrm{oc}}}^{T}\Delta T\Bigr)\Bigr)/V_{\mathrm{t}_{\mathrm{NOCTC}}}a_{\mathrm{NOCTC}}1\Bigr) - 1\Bigr]}.
\end{aligned}
\tag{37}
$$

By using the above equations and by applying the same procedure as is applied to find $R_{\mathrm{s}_{\mathrm{STC}}}$ and $R_{\mathrm{p}_{\mathrm{STC}}}$, $R_{\mathrm{s}_{\mathrm{NOCTC}}}$ and $R_{\mathrm{p}_{\mathrm{NOCTC}}}$ can be obtained.

$$
\begin{aligned}
R_{\mathrm{p}_{\mathrm{NOCTC}}}1 &= \frac{x}{y},\\
x &= \Bigl(\Bigl(1 + K_{V_{\mathrm{mpp}}}^{G}\Bigl(\log\Bigl(\frac{G_{\mathrm{NOCTC}}}{G_{\mathrm{STC}}}\Bigr)\Bigr)\Bigr)\Bigl(V_{\mathrm{mpp}_{\mathrm{STC}}} + K_{V_{\mathrm{mpp}}}^{T}\Delta T\Bigr)\Bigl(\Bigl(1 + K_{V_{\mathrm{mpp}}}^{G}\Bigl(\log\Bigl(\frac{G_{\mathrm{NOCTC}}}{G_{\mathrm{STC}}}\Bigr)\Bigr)\Bigr)\Bigl(V_{\mathrm{mpp}_{\mathrm{STC}}} + K_{V_{\mathrm{mpp}}}^{T}\Delta T\Bigr)\\
&\quad + \Bigl(\frac{G_{\mathrm{NOCTC}}}{G_{\mathrm{STC}}}\Bigl(I_{\mathrm{mpp}_{\mathrm{STC}}} + K_{I_{\mathrm{mpp}}}^{T}\Delta T\Bigr)R_{\mathrm{sNOCTC}}1\Bigr),\\
y &= \Bigl(\Bigl(1 + K_{V_{\mathrm{mpp}}}^{G}\Bigl(\log\Bigl(\frac{G_{\mathrm{NOCTC}}}{G_{\mathrm{STC}}}\Bigr)\Bigr)\Bigr)\Bigl(V_{\mathrm{mpp}_{\mathrm{STC}}} + K_{V_{\mathrm{mpp}}}^{T}\Delta T\Bigr)\Bigl(\frac{G_{\mathrm{NOCTC}}}{G_{\mathrm{STC}}}\Bigl(I_{\mathrm{sc}_{\mathrm{STC}}} + K_{I_{\mathrm{sc}}}^{T}\Delta T\Bigr)\Bigr)\Bigl(1 + \frac{R_{\mathrm{s}_{\mathrm{NOCTC}}}}{R_{\mathrm{p}_{\mathrm{NOCTC}}}}\Bigr)\Bigr)\\
&\quad - \Bigl(\Bigl(1 + K_{V_{\mathrm{mpp}}}^{G}\Bigl(\log\Bigl(\frac{G_{\mathrm{NOCTC}}}{G_{\mathrm{STC}}}\Bigr)\Bigr)\Bigr)\Bigl(V_{\mathrm{mpp}_{\mathrm{STC}}} + K_{V_{\mathrm{mpp}}}^{T}\Delta T\Bigr)\Bigr)\\
&\quad \cdot \Bigl(\frac{\Bigl(\Bigl(G_{\mathrm{NOCTC}}/G_{\mathrm{STC}}\Bigl(I_{\mathrm{sc}_{\mathrm{STC}}} + K_{I_{\mathrm{sc}}}^{T}\Delta T\Bigr)\Bigr)\Bigl(1 + \Bigl(R_{\mathrm{s}_{\mathrm{NOCTC}}}/R_{\mathrm{p}_{\mathrm{NOCTC}}}\Bigr)\Bigr)\Bigr) - \Bigl(\Bigl(\Bigl(\Bigl(1 + K_{V_{\mathrm{oc}}}^{G}(\log(G_{\mathrm{NOCTC}}/G_{\mathrm{STC}}))\Bigr)\Bigr)\Bigl(V_{\mathrm{oc}_{\mathrm{STC}}} + K_{V_{\mathrm{oc}}}^{T}\Delta T\Bigr)\Bigr)/R_{\mathrm{p}_{\mathrm{NOCTC}}}\Bigr)}{\Bigl[\exp\Bigl(\Bigl(\Bigl(1 + K_{V_{\mathrm{oc}}}^{G}(\log(G_{\mathrm{NOCTC}}/G_{\mathrm{STC}}))\Bigr)\Bigl(V_{\mathrm{oc}_{\mathrm{STC}}} + K_{V_{\mathrm{oc}}}^{T}\Delta T\Bigr)\Bigr)/V_{\mathrm{t}_{\mathrm{NOCTC}}}a_{\mathrm{NOCTC}}1\Bigr) - 1\Bigr]}\Bigr)\\
&\quad \cdot \exp\Bigl[\frac{\Bigl(\Bigl(1 + K_{V_{\mathrm{mpp}}}^{G}(\log(G_{\mathrm{NOCTC}}/G_{\mathrm{STC}}))\Bigr)\Bigl(V_{\mathrm{mpp}_{\mathrm{STC}}} + K_{V_{\mathrm{mpp}}}^{T}\Delta T\Bigr)\Bigr) + \Bigl(G_{\mathrm{NOCTC}}/G_{\mathrm{STC}}\Bigl(I_{\mathrm{mpp}_{\mathrm{STC}}} + K_{I_{\mathrm{mpp}}}^{T}\Delta T\Bigr)\Bigr)R_{\mathrm{s}_{\mathrm{NOCTC}}}1}{V_{\mathrm{t}_{\mathrm{NOCTC}}}a_{\mathrm{NOCTC}}1}\Bigr]\\
&\quad + \Bigl(\Bigl(1 + K_{V_{\mathrm{mpp}}}^{G}(\log(G_{\mathrm{NOCTC}}/G_{\mathrm{STC}}))\Bigr)\Bigl(V_{\mathrm{mpp}_{\mathrm{STC}}} + K_{V_{\mathrm{mpp}}}^{T}\Delta T\Bigr)\Bigr)\\
&\quad \cdot \Bigl(\frac{\Bigl(\Bigl(G_{\mathrm{NOCTC}}/G_{\mathrm{STC}}\Bigl(I_{\mathrm{sc}_{\mathrm{STC}}} + K_{I_{\mathrm{sc}}}^{T}\Delta T\Bigr)\Bigr)\Bigl(1 + \Bigl(R_{\mathrm{s}_{\mathrm{NOCTC}}}/R_{\mathrm{p}_{\mathrm{NOCTC}}}\Bigr)\Bigr)\Bigr) - \Bigl(\Bigl(\Bigl(1 + K_{V_{\mathrm{oc}}}^{G}(\log(G_{\mathrm{NOCTC}}/G_{\mathrm{STC}}))\Bigr)\Bigl(V_{\mathrm{oc}_{\mathrm{STC}}} + K_{V_{\mathrm{oc}}}^{T}\Delta T\Bigr)\Bigr)/R_{\mathrm{p}_{\mathrm{NOCTC}}}\Bigr)}{\Bigl[\exp\Bigl(\Bigl(\Bigl(1 + K_{V_{\mathrm{oc}}}^{G}(\log(G_{\mathrm{NOCTC}}/G_{\mathrm{STC}}))\Bigr)\Bigl(V_{\mathrm{oc}_{\mathrm{STC}}} + K_{V_{\mathrm{oc}}}^{T}\Delta T\Bigr)\Bigr)/V_{\mathrm{t}_{\mathrm{NOCTC}}}a_{\mathrm{NOCTC}}1\Bigr) - 1\Bigr]}\Bigr)\\
&\quad - \Bigl(\frac{G_{\mathrm{NOCTC}}}{G_{\mathrm{STC}}}\Bigl(1 + K_{P_{\mathrm{mpp}}}^{G}\Bigl(\log\Bigl(\frac{G_{\mathrm{NOCTC}}}{G_{\mathrm{STC}}}\Bigr)\Bigr)\Bigr)\Bigl(P_{\mathrm{mpp}_{\mathrm{STC}}} + K_{P_{\mathrm{mpp}}}^{T}\Delta T\Bigr)\Bigr).
\end{aligned}
\tag{38}
$$

Table 2: First level of improved values of the parameters of seven different commercially available PV modules for the proposed model and evaluated parameters of seven different commercially available PV modules for the R_s model, R_s and R_p model, and two-diode model at STC.

Model	Parameter	Thin film		Monocrystalline			Multicrystalline	
		Shell ST40	FS-270	Shell SQ 150-PC	HIT-N240SE10	KD140GX-LFBS	KD260GX-LFB2	KU265-6MCA
Proposed model	$I_{pv_{STC}}$ A	2.68	1.23	4.80	5.85	8.68	9.09	9.26
	a_{STC}	1.61421	3.10639	1.56173	1.41612	1.83175	1.63175	1.62276
	$I_{0_{STC}}$ A	4.4733×10^{-7}	9.1598×10^{-5}	1.4356×10^{-6}	1.2024×10^{-8}	1.8772×10^{-5}	2.2181×10^{-6}	2.0768×10^{-6}
	$R_{s_{STC}}$ Ω	1.35870	3.45266	0.45588	0.25077	0.03751	0.10264	0.10303
	$R_{p_{STC}}$ Ω	139391.478	1791835.933	2123.494	405454010.026	485618.624	2135142.579	710599.657
	$I_{pv_{STC}}1$ A	2.680026122	1.230002370	4.801030482	5.849999758	8.680000670	9.089999904	9.260001342
	$a_{STC}1$	1.61343	3.10212	1.51490	1.41164	1.83159	1.63119	1.62237
	$I_{0_{STC}}1$ A	4.4395×10^{-7}	9.0404×10^{-5}	8.9866×10^{-7}	1.1284×10^{-8}	1.8751×10^{-5}	2.2066×10^{-6}	2.0692×10^{-6}
	$R_{s_{STC}}1$ Ω	1.35915	3.46672	0.48855	0.25478	0.03754	0.10286	0.10315
	$R_{p_{STC}}1$ Ω	69436.135	295078.680	1219.87237	330003.053	185988.578	324974.945	161649.074
	$a_{STC}2$	1.61267	3.09829	1.46550	1.41036	1.83143	1.63088	1.62201
R_s model	$I_{pv_{STC}}$ A	2.68	1.23000	4.80	5.85	8.68	9.09	9.26
	a_{STC}	1.22997	1.10571	1.05938	1.06008	1.06425	1.10663	1.10663
	$I_{0_{STC}}$ A	3.4150×10^{-9}	3.10874×10^{-12}	1.1570×10^{-9}	1.4537×10^{-11}	1.5423×10^{-9}	1.6151×10^{-9}	1.6453×10^{-9}
	$R_{s_{STC}}$ Ω	1.69665	14.74644	1.02961	0.56631	0.25480	0.34877	0.34138
R_s and R_p model	$I_{pv_{STC}}$ A	2.68	1.23000	4.80	5.85	8.68	9.09	9.26
	a_{STC}	1.22997	1.10571	1.05938	1.06008	1.06425	1.10663	1.10663
	$I_{0_{STC}}$ A	3.4150×10^{-9}	3.10874×10^{-12}	1.1570×10^{-9}	1.4537×10^{-11}	1.5423×10^{-9}	1.6151×10^{-9}	1.6453×10^{-9}
	$R_{s_{STC}}$ Ω	1.54000	11.61000	0.83200	0.43700	0.17800	0.27400	0.26900
	$R_{p_{STC}}$ Ω	266.37955	762.36643	262.75328	445.13305	53.88571	154.59042	154.15067
Two-diode model	$I_{pv_{STC}}$ A	2.68	1.23000	4.80	5.85	8.68	9.09	9.26
	$a1_{STC}$	1.00000	1.00000	1.00000	1.00000	1.00000	1.00000	1.00000
	$a2_{STC}$	1.20000	1.20000	1.20000	1.20000	1.20000	1.20000	1.20000
	$I_{0_{STC}}$ A	3.0748×10^{-11}	1.847458×10^{-13}	3.1059×10^{-10}	2.9186×10^{-12}	3.6446×10^{-10}	1.4740×10^{-10}	1.5016×10^{-10}
	$R_{s_{STC}}$ Ω	1.71000	12.18000	0.90000	0.50000	0.20000	0.31000	0.30000
	$R_{p_{STC}}$ Ω	204.84910	726.87888	274.79210	458.96360	55.92360	130.55740	124.58140

Table 3: Evaluated irradiance coefficients of V_{oc}, $V_{mpp,}$ and P_{mpp} of seven different commercially available PV modules and evaluated parameters of seven different commercially available PV modules at NOCTC (45°C and 1000 W/m^2) for the proposed model.

Model	Parameter	Thin film		Monocrystalline			Multicrystalline	
		Shell ST40	FS-270	Shell SQ 150-PC	HIT-N240SE10	KD140GX-LFBS	KD260GX-LFB2	KU265-6MCA
Proposed model	$K^G_{V_{oc}}$	0.084956	0.096490	0.046921	0.045882	0.067477	0.055781	0.055781
	$K^G_{V_{mpp}}$	−0.093363	−0.022004	−0.074512	0.012071	−0.039787	0.019829	0.019829
	$K^G_{P_{mpp}}$	0.012262	0.058966	−0.046283	−0.023365	0.030671	0.053982	0.044600
	$I_{pv_{NOCTC}}$ A	2.150160000	0.991872000	3.863519999	4.706751999	7.027328000	7.359264000	7.496895999
	a_{NOCTC}	1.75584	2.86595	1.67257	1.21016	1.74535	1.50015	1.49252
	$I_{0_{NOCTC}}$ A	1.5043×10^{-5}	1.2555×10^{-4}	2.4789×10^{-5}	4.6055×10^{-9}	5.6770×10^{-5}	4.8923×10^{-6}	4.6342×10^{-6}
	$R_{s_{NOCTC}}$ Ω	1.21772	2.40133	0.24346	0.33097	0.02807	0.15316	0.14925
	$R_{p_{NOCTC}}$ Ω	1881.9879	14942.890	4073.0256	3790.1388	469.1091	552.7469	644.3563

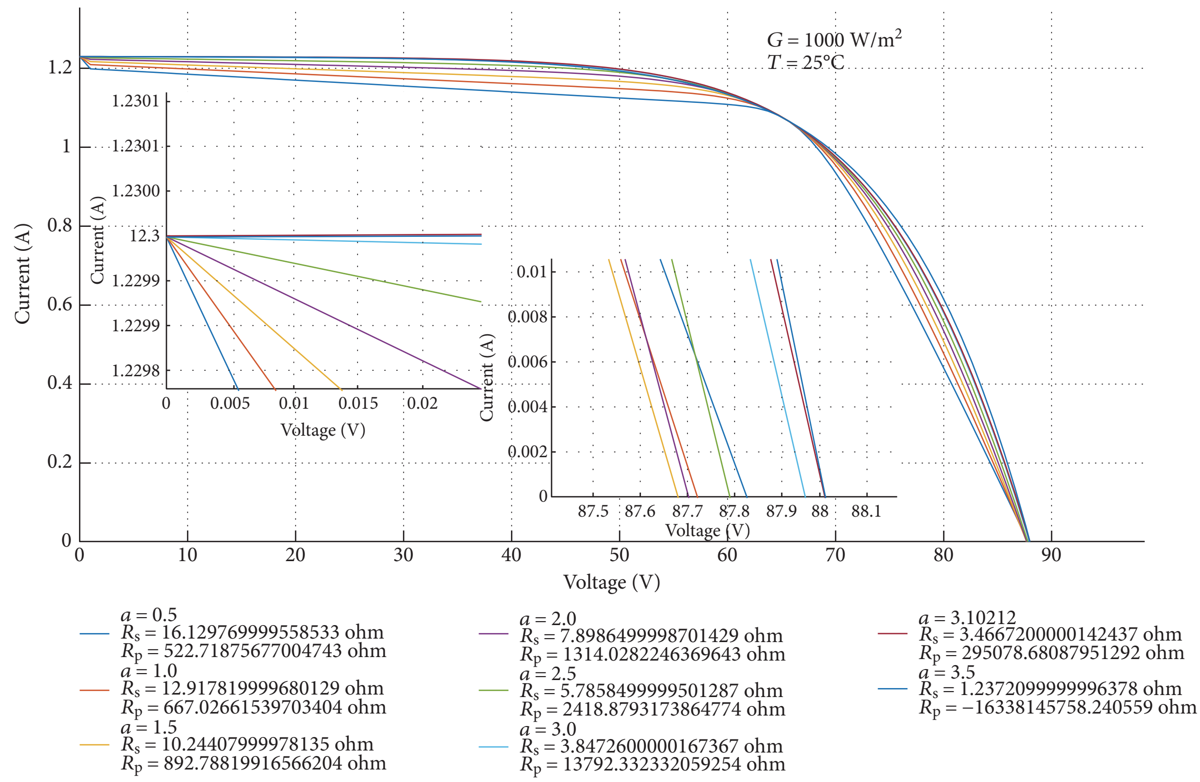

(a) *I-V* characteristics

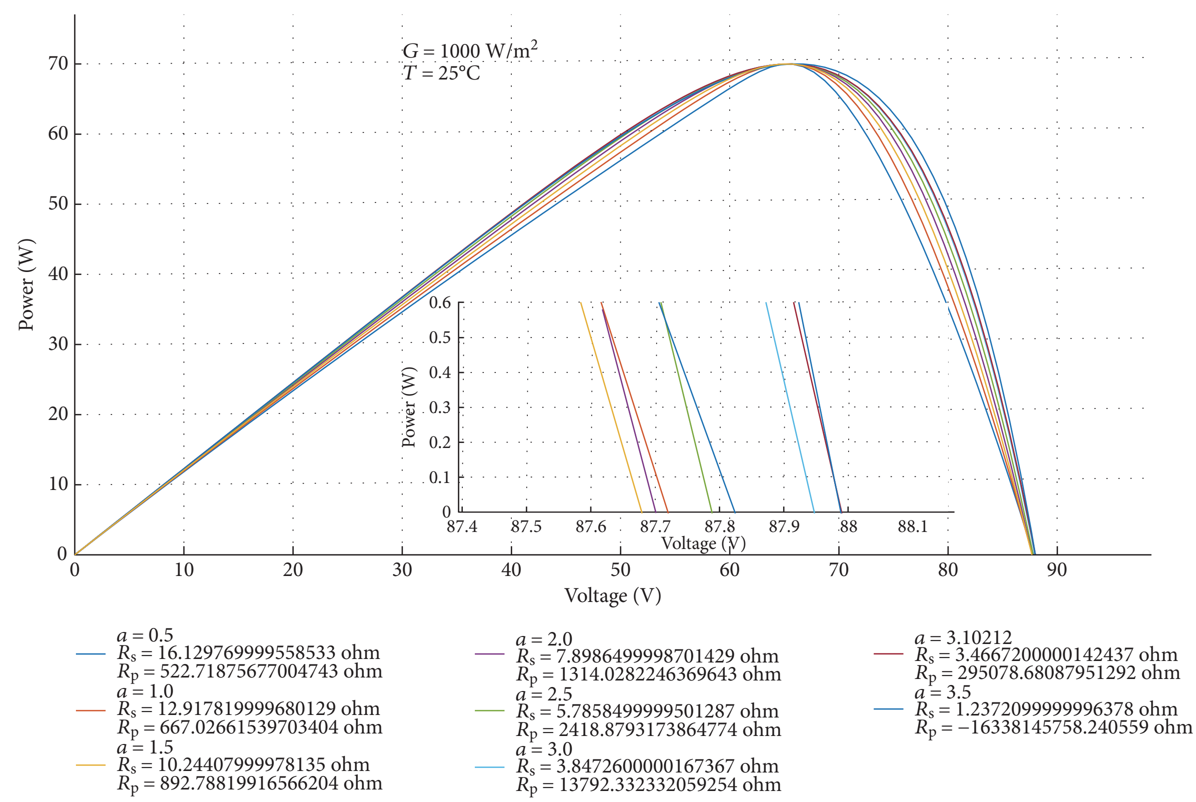

(b) *P-V* characteristics

FIGURE 3: Characteristics for eight values of a_{STC} and the corresponding values of $R_{s_{STC}}$ and $R_{p_{STC}}$ of the FS-270 PV module at 25°C and 1000 W/m^2.

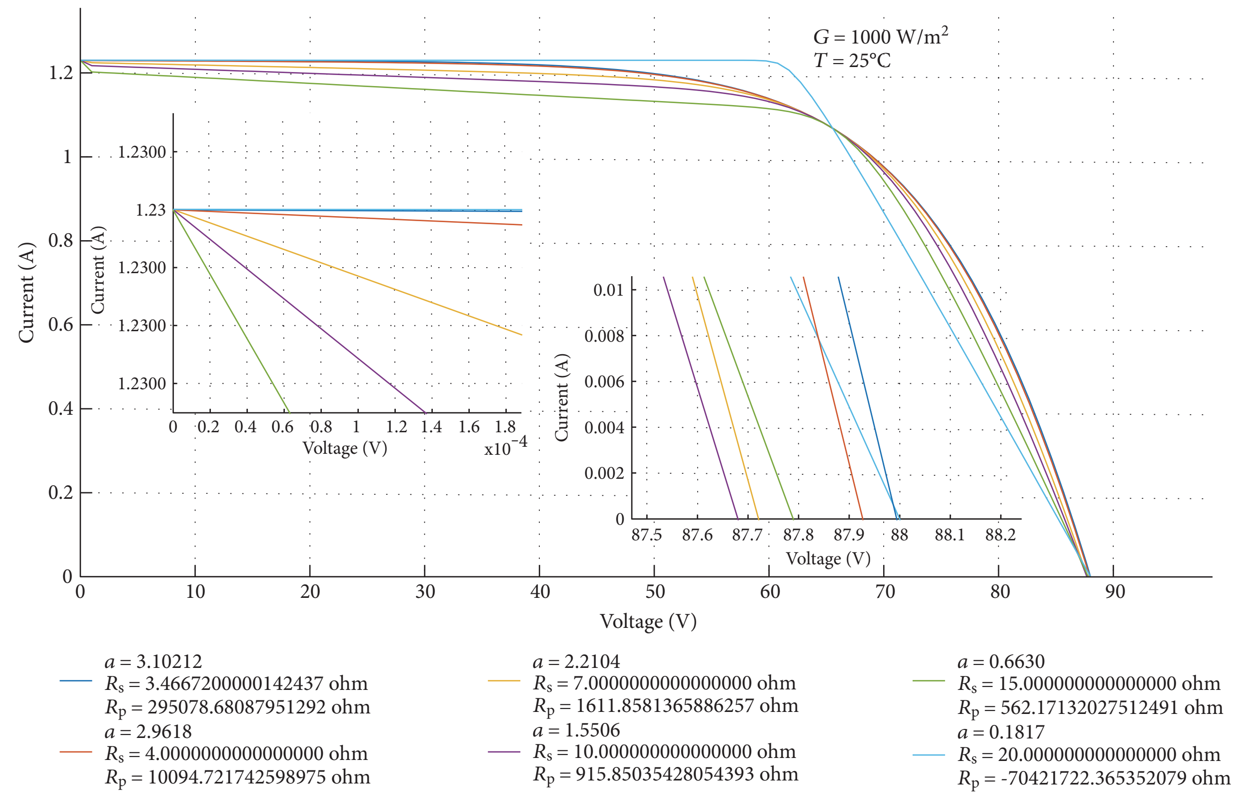

(a) *I-V* characteristics

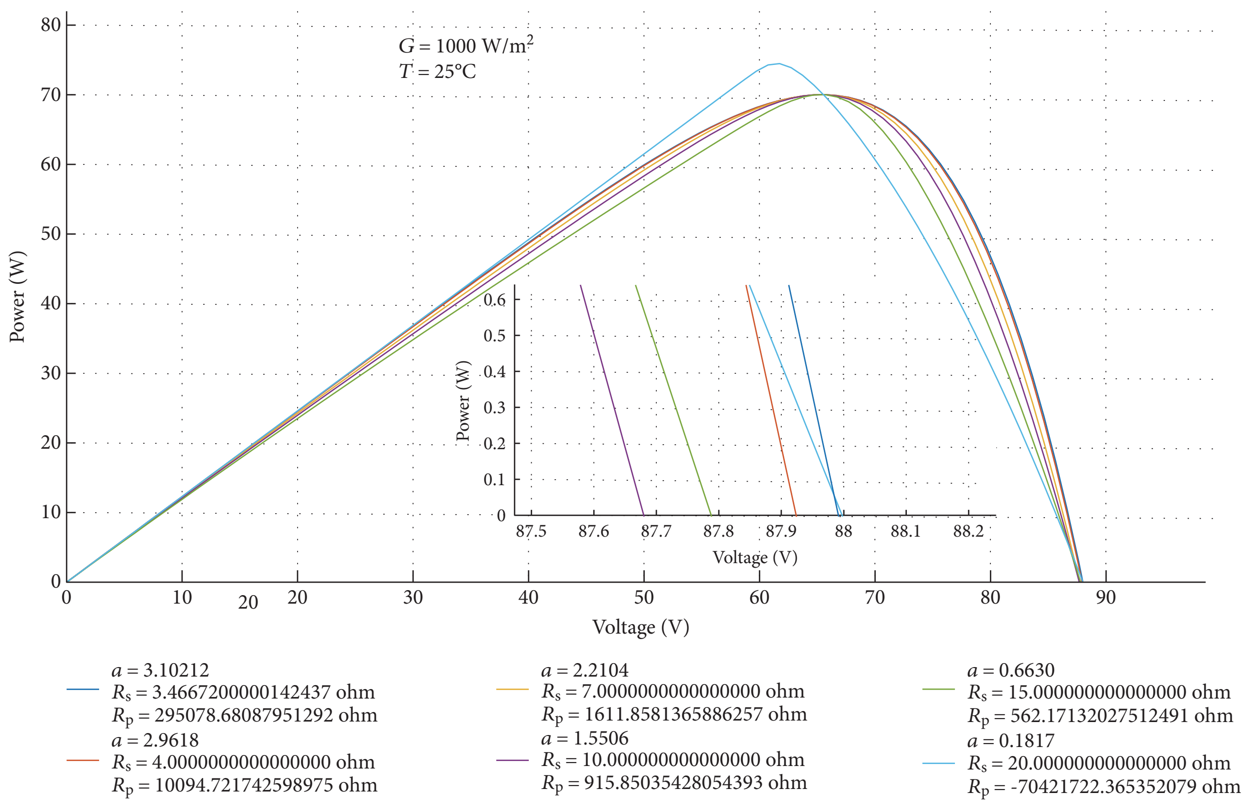

(b) *P-V* characteristics

FIGURE 4: Characteristics for six values of $R_{s_{STC}}$ and the corresponding values of a_{STC} and $R_{p_{STC}}$ of the FS-270 PV module at 25°C and 1000 W/m^2.

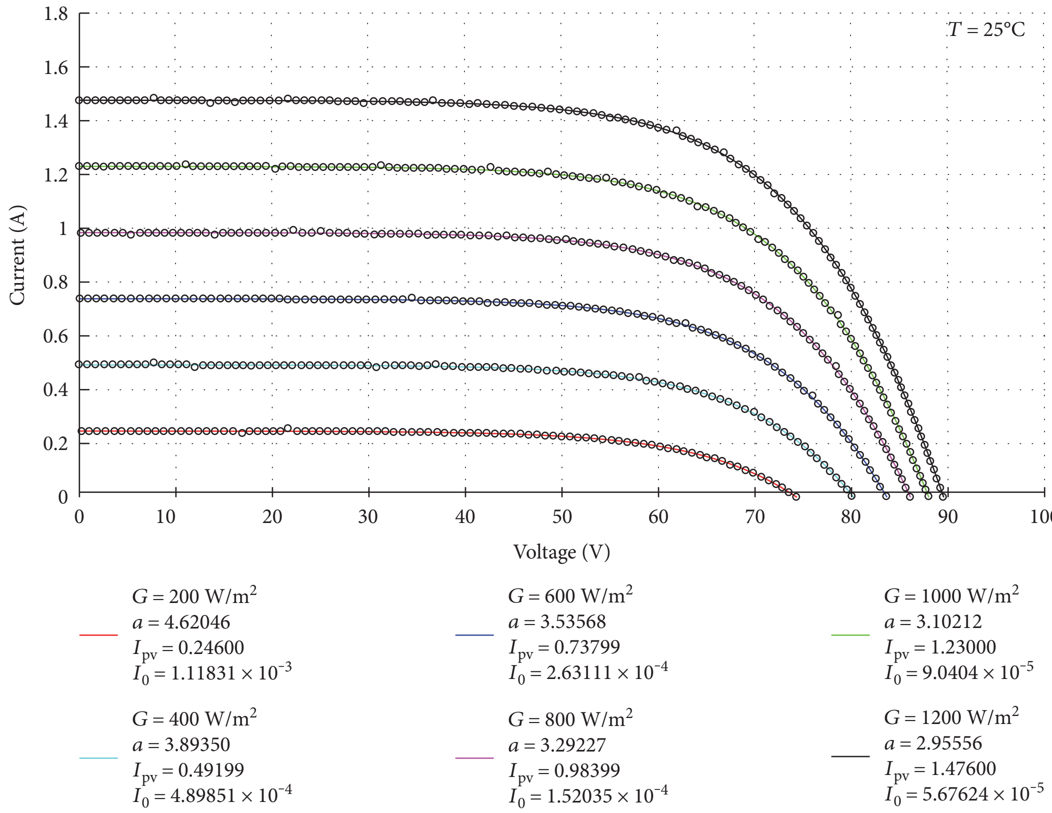

(a) *I-V* characteristics

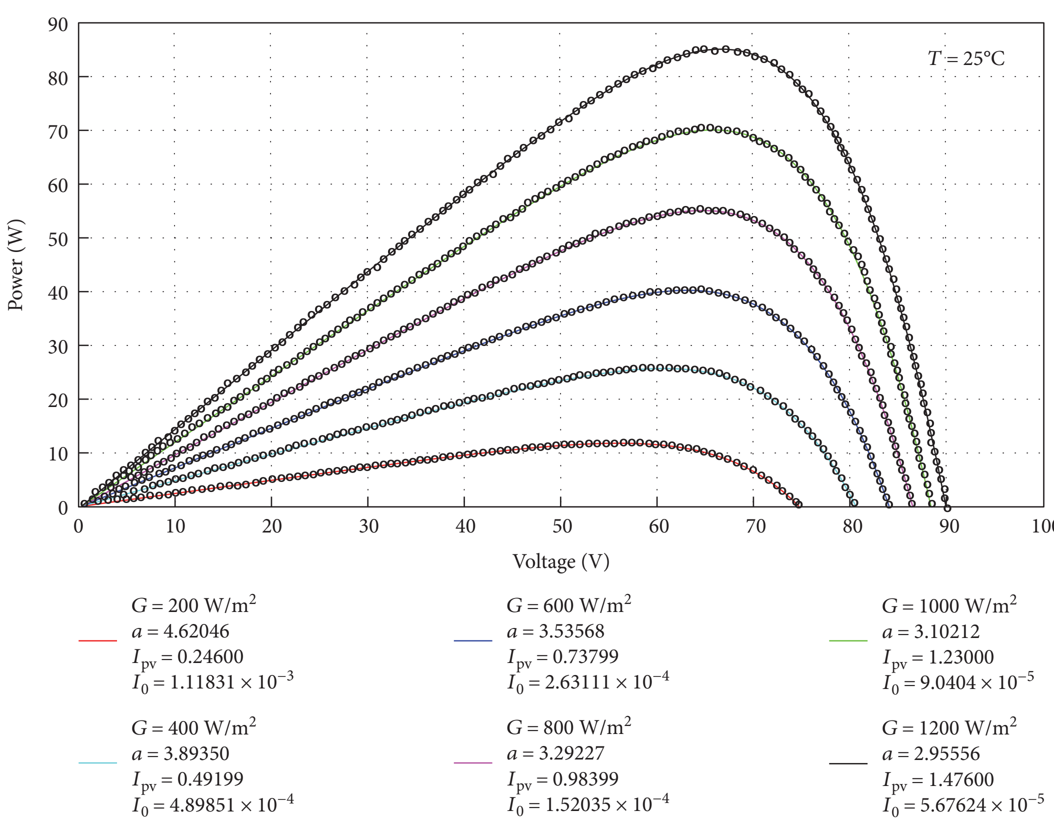

(b) *P-V* characteristics

FIGURE 5: Characteristics and experimental data of the FS-270 PV module at different irradiances (temperature constant = 25°C).

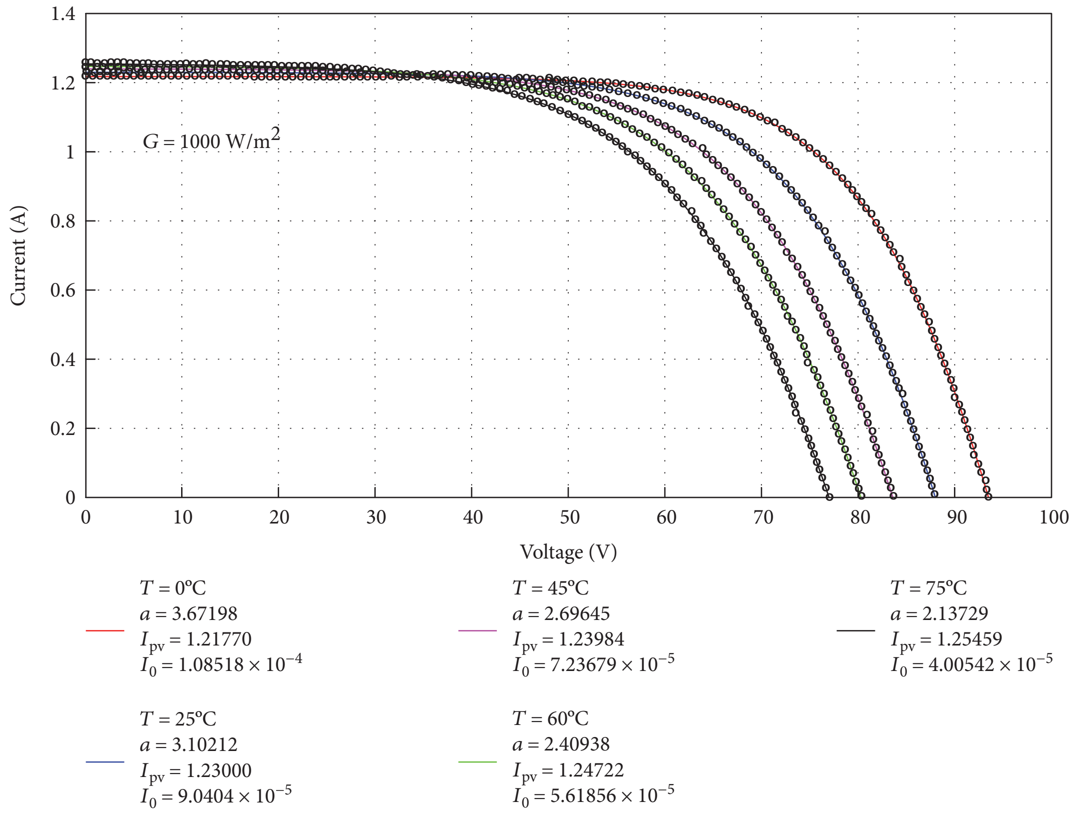

(a) *I-V* characteristics

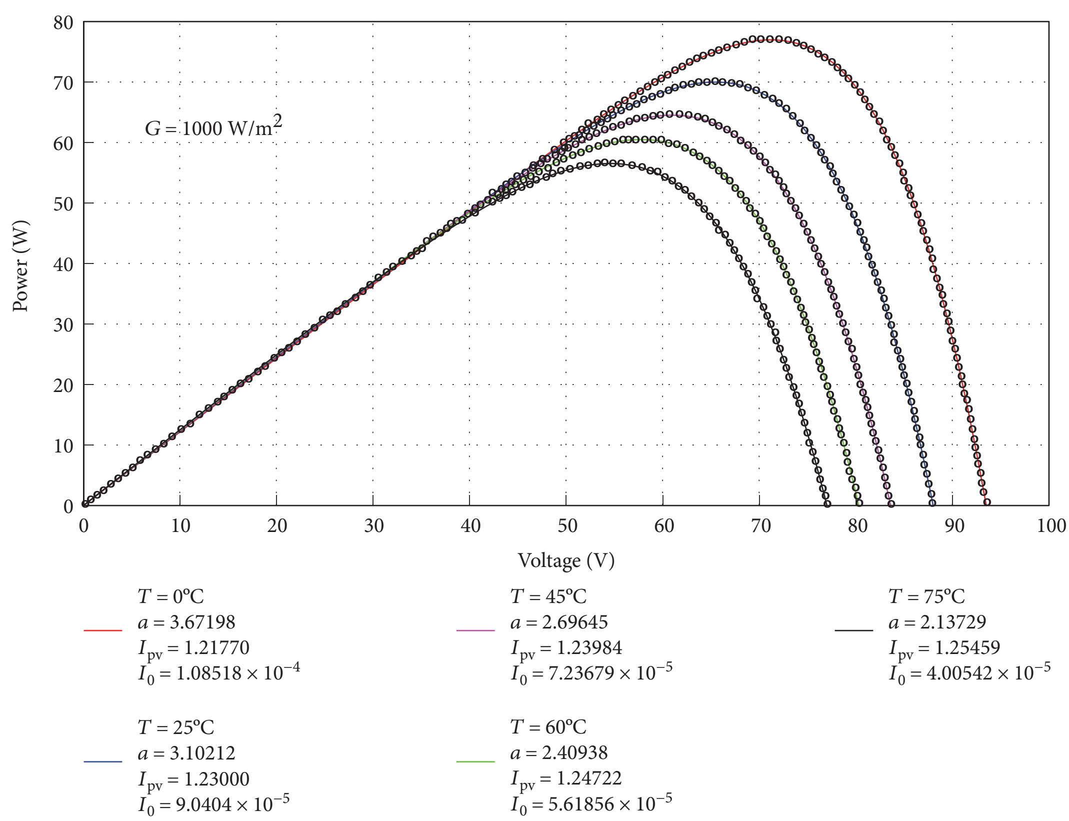

(b) *P-V* characteristics

Figure 6: Characteristics and experimental data of the FS-270 PV module at different temperatures (irradiance constant = 1000 W/m^2).

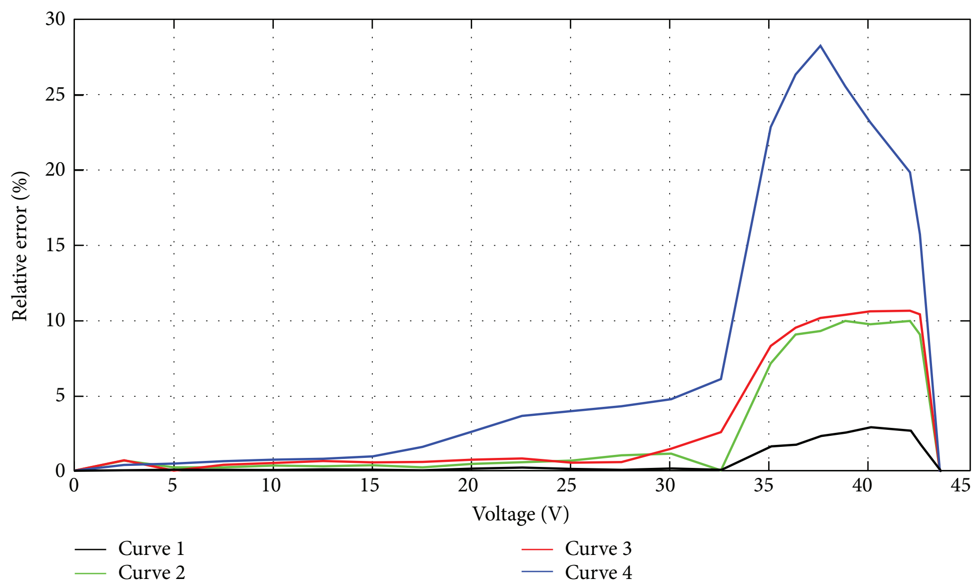

Figure 7: Relative errors of the model proposed in this paper (curve 1), in [4] (curve 2), in [12] (curve 3), and in [6] (curve 4) for the FS-270 PV module at 25°C and 1000 W/m^2.

Table 4: Comparison of R_s model, R_s and R_p model, two-diode model, and proposed model output with manufacturer's datasheet for Shell ST40 PV module [30].

Environmental conditions	Parameter	Datasheet value	R_s model value	R_s and R_p model value	Two-diode model value	Proposed model value	Error R_s (%)	Error R_s and R_p (%)	Error two-diode (%)	Error proposed (%)
STC (**25**°C and **1000** W/m^2)	P_{mpp} W	40	29.0224	40.0055	40.0060	40.0000	−27.4589	−0.0012	0.0150	0.0000
	V_{mpp} V	16.6	14.9120	16.7760	16.6000	16.6029	−10.1686	1.0602	0.0000	0.0174
	I_{mpp} A	2.41	1.9462	2.3847	2.4100	2.4098	−19.2448	−1.0497	0.0000	−0.0082
	V_{oc} V	23.3	21.0254	23.2618	23.2460	23.2993	−9.7622	−0.1639	−0.2317	−0.0030
	I_{sc} A	2.68	2.1590	2.6646	2.6578	2.6800	−19.4402	−0.5746	−0.8283	0.0000
NOCTC (**47**°C and **800** W/m^2)	P_{mpp} W	27.7	19.5088	28.2982	28.5162	27.7024	−29.5711	2.1595	2.9465	0.0086
	V_{mpp} V	14.7	12.6790	14.9120	14.9120	14.6933	−13.7482	1.4421	1.4421	−0.0455
	V_{oc} V	20.7	18.8271	20.7820	20.8002	20.7009	−9.0478	0.3961	0.4840	0.0043
	I_{sc} A	2.2	1.7502	2.1378	2.1324	2.1982	−20.4454	−2.8272	−3.0727	−0.0818

Table 5: Comparison of R_s model, R_s and R_p model, two-diode model, and proposed model output with manufacturer's datasheet for Shell SQ 150-PC PV module [32].

Environmental conditions	Parameter	Datasheet value	R_s model value	R_s and R_p model value	Two-diode model value	Proposed model value	Error R_s (%)	Error R_s and R_p (%)	Error two-diode (%)	Error proposed (%)
STC (**25**°C and **1000** W/m^2)	P_{mpp} W	150	111.6218	149.5998	149.6000	150.0000	−25.5854	−0.2668	−0.2666	0.0000
	V_{mpp} V	34	30.3800	34.2860	34.0000	34.0115	−10.6470	0.8411	0.0000	0.0338
	I_{mpp} A	4.4	3.6742	4.3633	4.4000	4.3998	−16.4954	−0.8340	0.0000	−0.0045
	V_{oc} V	43.4	39.7399	43.3302	43.3012	43.3972	−8.4334	−0.1608	−0.2276	−0.0064
	I_{sc} A	4.8	3.9475	4.7848	4.7843	4.8000	−17.7604	−0.3166	−0.3270	0.0000
NOCTC (46°C and 800 W/m^2)	P_{mpp} W	108	85.7801	107.7001	107.8484	107.9950	−20.5739	−0.2776	−0.1403	−0.0046
	V_{mpp} V	31	26.3800	30.8140	30.8140	30.9800	−14.9032	−0.5999	−0.5999	−0.0645
	V_{oc} V	39.6	36.4498	39.4670	39.4310	39.5964	−7.9550	−0.3358	−0.4267	−0.0090
	I_{sc} A	3.9	3.3635	3.8513	3.8509	3.8985	−13.7564	−1.2487	−1.2589	−0.0384

Table 6: Comparison of R_s model, R_s and R_p model, two-diode model, and proposed model output with manufacturer's datasheet for HIT-N240SE10 PV module [33].

Environmental conditions	Parameter	Datasheet value	R_s model value	R_s and R_p model value	Two-diode model value	Proposed model value	Error R_s (%)	Error R_s and R_p (%)	Error two-diode (%)	Error proposed (%)
STC (**25**°C and **1000** W/m^2)	P_{mpp} W	240	186.2506	240.7864	240.7870	240.0000	−22.3955	0.3276	0.3279	0.0000
	V_{mpp} V	43.7	40.8720	44.0160	43.7000	43.7008	−6.4713	0.7231	0.0000	0.0018
	I_{mpp} A	5.51	4.5569	5.4704	5.5100	5.5096	−17.2976	−0.7186	0.0000	−0.0072
	V_{oc} V	52.4	49.3547	52.3588	52.3470	52.3988	−5.8116	−0.0786	−0.1011	−0.0022
	I_{sc} A	5.85	4.8447	5.8443	5.8436	5.8500	−17.1846	−0.0974	−0.1094	0.0000
NOCTC (44°C and 800 W/m^2)	P_{mpp} W	182	149.8145	180.5653	180.9046	181.9713	−17.6843	−0.7882	−0.6018	−0.0157
	V_{mpp} V	41.1	37.8720	41.3960	41.3960	41.0970	−7.8540	0.7201	0.7201	−0.0072
	I_{mpp} A	4.44	3.6484	4.3619	4.3701	4.4396	−17.8288	−1.7590	−1.5743	−0.0090
	V_{oc} V	49.4	45.5426	49.3914	49.3938	49.3992	−7.8085	−0.0174	−0.0125	−0.0016
	I_{sc} A	4.71	3.8068	4.7021	4.7016	4.7098	−19.1762	−0.1677	−0.1783	−0.0042

Table 7: Comparison of R_s model, R_s and R_p model, two-diode model, and proposed model output with manufacturer's datasheet for KD140GX-LFBS PV module [34].

Environmental conditions	Parameter	Datasheet value	R_s model value	R_s and R_p model value	Two-diode model value	Proposed model value	Error R_s (%)	Error R_s and R_p (%)	Error two-diode (%)	Error proposed (%)
STC (**25**°C and **1000** W/m^2)	P_{mpp} W	140	112.2240	139.9971	140.0070	140.0000	−19.8399	−0.0020	0.0050	0.0000
	V_{mpp} V	17.7	15.9120	17.9010	17.7000	17.7007	−10.1016	1.1355	0.0000	0.0039
	I_{mpp} A	7.91	7.0528	7.8206	7.9100	7.9091	−10.8369	−1.1302	0.0000	−0.0113
	V_{oc} V	22.1	20.3590	22.0514	22.0396	22.1000	−7.8778	−0.2199	−0.2733	0.0000
	I_{sc} A	8.68	7.6673	8.6514	8.6491	8.6800	−11.6670	−0.3294	−0.3559	0.0000
NOCTC (45°C and 800 W/m^2)	P_{mpp} W	101	79.3291	101.7994	101.9756	100.9936	−21.4563	0.7914	0.9659	−0.0063
	V_{mpp} V	16.0	14.6910	16.1330	16.1330	15.9880	−8.1812	0.8312	0.8312	−0.0750
	I_{mpp} A	6.33	5.5852	6.3100	6.3209	6.3278	−11.7661	−0.3159	−0.1437	−0.0347
	V_{oc} V	20.2	18.0738	20.2155	20.2034	20.1983	−10.5257	0.0767	0.0168	−0.0084
	I_{sc} A	7.03	6.4273	7.0042	7.0023	7.0293	−8.5732	−0.3669	−0.3940	−0.0099

Table 8: Comparison of R_s model, R_s and R_p model, two-diode model, and proposed model output with manufacturer's datasheet for KD260GX-LFB2 PV module [35].

Environmental conditions	Parameter	Datasheet value	R_s model value	R_s and R_p model value	Two-diode model value	Proposed model value	Error R_s (%)	Error R_s and R_p (%)	Error two-diode (%)	Error proposed (%)
STC (**25**°C and **1000** W/m^2)	P_{mpp} W	260	208.7319	260.0899	260.0900	260.0000	−19.7185	0.0345	0.0346	0.0000
	V_{mpp} V	31.0	27.5760	31.0230	31.0000	31.0022	−11.0451	0.0741	0.0000	0.0070
	I_{mpp} A	8.39	7.5693	8.3838	8.3900	8.3895	−9.7818	−0.0738	0.0000	−0.0059
	V_{oc} V	38.3	35.2913	38.2471	38.2249	38.2994	−7.8556	−0.1381	−0.1960	−0.0015
	I_{sc} A	9.09	8.0652	9.0739	9.0685	9.0900	−11.2739	−0.1771	−0.2365	0.0000
NOCTC (45°C and 800 W/m^2)	P_{mpp} W	187	142.6852	189.3933	189.8687	186.9801	−23.6977	1.2798	1.5340	−0.0106
	V_{mpp} V	27.9	24.7590	28.3420	28.3420	27.8997	−11.2580	1.5842	1.5842	−0.0010
	I_{mpp} A	6.71	5.8309	6.6824	6.6992	6.7096	−13.1013	−0.4113	−0.1609	−0.0059
	V_{oc} V	35.1	33.8348	35.0769	35.0657	35.0982	−3.6045	−0.0658	−0.0977	−0.0051
	I_{sc} A	7.36	6.1593	7.3462	7.3418	7.3597	−16.3138	−0.1875	−0.2472	−0.0040

Table 9: Comparison of R_s model, R_s and R_p model, two-diode model, and proposed model output with manufacturer's datasheet for KU265-6MCA PV module [36].

Environmental conditions	Parameter	Datasheet value	R_s model value	R_s and R_p model value	Two-diode model value	Proposed model value	Error R_s (%)	Error R_s and R_p (%)	Error two-diode (%)	Error proposed (%)
STC (**25**°C and **1000** W/m^2)	P_{mpp} W	265	213.0696	265.0499	265.0500	265.0000	−19.5963	0.0188	0.0188	0.0000
	V_{mpp} V	31.0	27.5760	31.0230	31.0000	31.0030	−11.0451	0.0741	0.0000	0.0096
	I_{mpp} A	8.55	7.7266	8.5437	8.5500	8.5490	−9.6304	−0.0736	0.0000	−0.0116
	V_{oc} V	38.3	35.2946	38.2529	38.2234	38.3000	−7.8469	−0.1229	−0.1999	0.0000
	I_{sc} A	9.26	8.2312	9.2439	9.2378	9.2600	−11.1101	−0.1738	−0.2397	0.0000
NOCTC (45°C and 800 W/m^2)	P_{mpp} W	191	147.6087	193.0154	193.4476	190.9769	−22.7179	1.0551	1.2814	−0.0120
	V_{mpp} V	27.9	24.5590	28.3420	28.3420	27.8975	−11.9749	1.5842	1.5842	−0.0089
	I_{mpp} A	6.85	5.5069	6.8102	6.8255	6.8496	−19.6072	−0.5810	−0.3576	−0.0058
	V_{oc} V	35.1	33.6348	35.0778	35.0639	35.0975	−4.1743	−0.0632	−0.1028	−0.0071
	I_{sc} A	7.49	6.9605	7.4838	7.4789	7.4902	−7.0694	−0.0827	−0.1481	0.0026

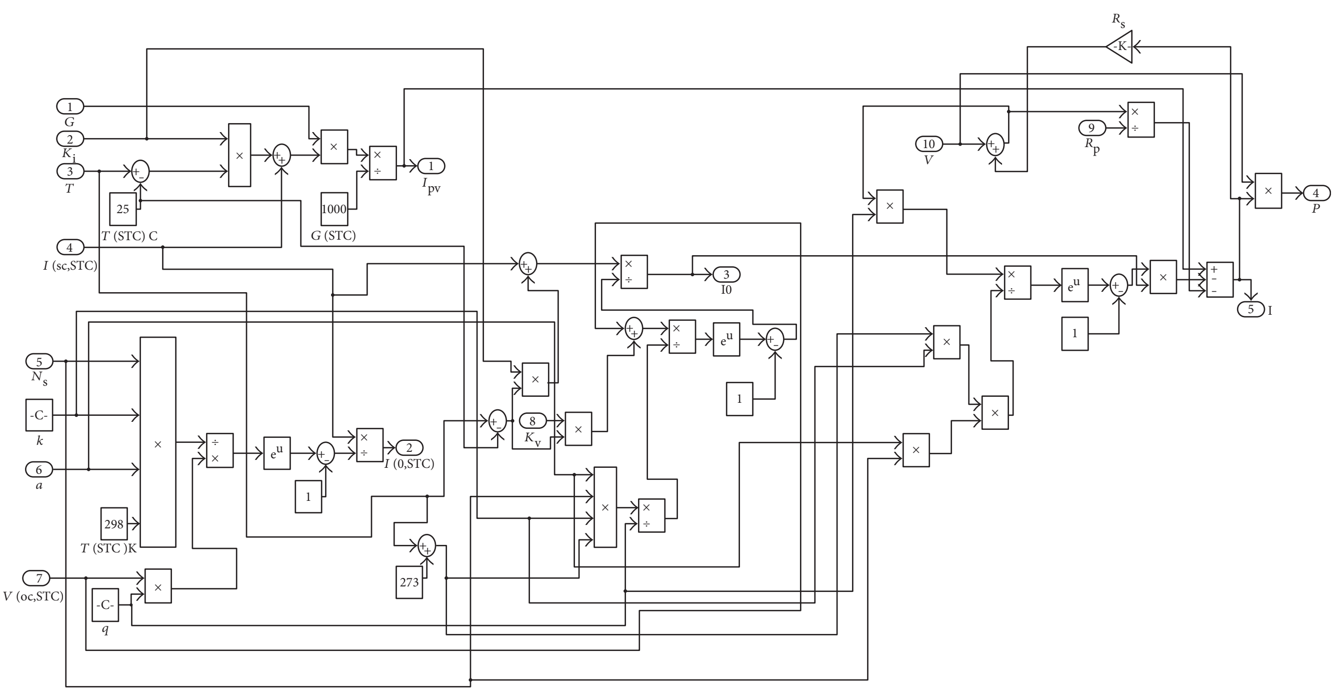

Figure 8: Detailed implementation of PV module model in MATLAB/Simulink that solves the *I*-*V* equation.

Table 3 shows the evaluated irradiance coefficients of V_{oc}, V_{mpp}, and P_{mpp} of seven different commercially available PV modules and evaluated parameters of seven different commercially available PV modules at NOCTC for the proposed model.

It is evident from the above equations that all the parameters of the characteristic equation of the PV module are subject to vary with irradiance and temperature, which is a truism. This increases the accuracy of the proposed method of evaluating parameters manifold as compared to existing methods in this area where the parameters are assumed constant [4, 6, 12]. The proposed model output characteristics very accurately match the experimental output characteristics and manufacturer's datasheets which is authenticated from the results shown in the later sections.

8. Curves and Inferences

As shown in Figures 3(a) and 3(b), *I*-*V* and *P*-*V* curves of the FS-270 PV module are generated for eight values of a_{STC} and the corresponding values of $R_{s_{STC}}$ and $R_{p_{STC}}$. It can be noted that as the value of a_{STC} calculated by the proposed method is utilised, the value of $V_{oc_{STC}}$ obtained from the proposed model becomes closest to the datasheet value. *I*-*V* and *P*-*V* curves of the FS-270 PV module are plotted again for six values of $R_{s_{STC}}$ and the corresponding values of a_{STC} and

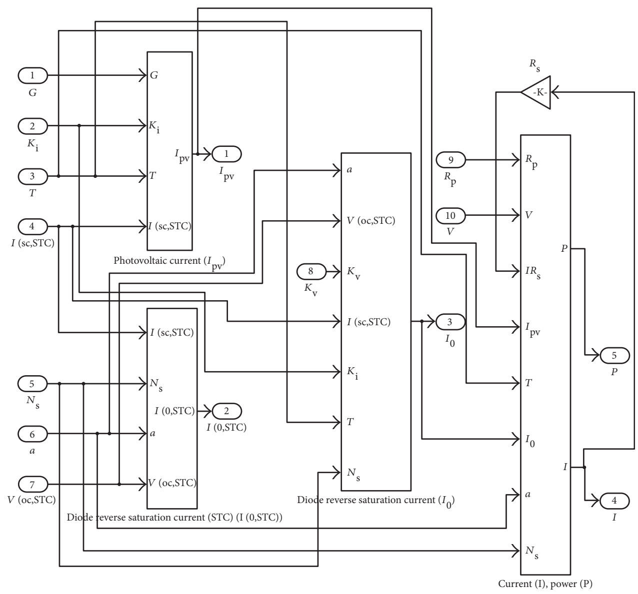

Figure 9: PV module model with subsystems in MATLAB/Simulink that solves the *I-V* equation.

$R_{p_{STC}}$ (see Figures 4(a) and 4(b)). As the value of $R_{s_{STC}}$ calculated by the proposed method is utilised, the value of $V_{oc_{STC}}$ obtained from the proposed model becomes closest to the datasheet value. Similar is the case with $R_{p_{STC}}$. The accuracy of the model is highest, when the values of a_{STC}, $R_{s_{STC}}$, and $R_{p_{STC}}$ calculated by the proposed technique are utilised for modeling. The proposed method of evaluating the unknown parameters is far more accurate as compared to other methods mentioned in literature.

9. Validation of the Model

The current and power output obtained from the proposed model is validated against measured current and power output data, respectively, for the FS-270 PV module provided by the National Institute of Technology Patna (NITP), India.

Figures 5(a) and 5(b) show the mathematical *I-V* and *P-V* characteristics of the FS-270 PV module [31] plotted with the experimental data by varying irradiance from 200 W/m^2 to 1200 W/m^2 at 25°C. Figures 6(a) and 6(b) show the *I-V* and *P-V* curves by varying temperature from 0°C to 75°C at 1000 W/m^2. The experimental points are represented by circular markers in the curves. As the model is not perfect, some points are not exactly matched, although it is sufficiently accurate for majority points.

The relative errors of the proposed model with respect to the experimental data for the FS-270 PV module at 25°C and 1000 W/m^2 are shown in Figure 7. The model proposed in this paper is compared with the models proposed in [4, 6, 12]. The relative errors obtained by all the models are plotted on the same graphs. The model proposed in this paper is superior, because the values of relative errors obtained by the proposed model are very small as compared to other models.

Tables 4–9 show the comparison of R_s model, R_s and R_p model, two-diode model, and proposed model output with manufacturer's datasheets for six different commercially available PV modules [30–36].

In the proposed method, it has been assumed that all the PV cells of a module are perfectly made but this is not the case in reality. Still the proposed method confirms to be very accurate as can be clearly seen from Figure 7 and Tables 4–9. This is because the properties of the PV cells having the same parameters, manufactured from the same producer, do not vary much and hence can be assumed identical.

10. Simulation of the PV Module

The PV module model can be simulated in any circuit simulator by implementing (1) and (4) using basic math blocks. Figures 8 and 9 show a PV module model, where these two equations are implemented in MATLAB/Simulink. In the complete model, irradiance and temperature along with the evaluated and manufacturer-specified parameters of the PV module are the inputs while the outputs are current and power. The proposed model is most generalized as compared to the models proposed in previous works.

11. Conclusion

In this paper, an improved generalized method for evaluation of parameters, modeling, and simulation of photovoltaic modules is proposed.

The proposed PV module modeling method surpasses the other methods already published, as it has the following novelties:

(i) A new concept "Level of Improvement" has been proposed for evaluating unknown parameters of the nonlinear *I-V* equation of the single-diode model of PV module at any environmental condition (STC and NOCTC in this paper), taking the manufacturer-specified data at Standard Test Conditions as inputs.

(ii) The new method of evaluation of unknown parameters is based on mathematical equations of PV modules. By implementing simple set of equations using any software, the parameters can be determined numerically simply by feeding few manufacturer-specified data as input to the program.

(iii) In this paper, for the first time, the effects of varying ideality factor and resistances on the output curves have been observed. It has been inferred that as the values of a_{STC}, $R_{s_{STC}}$, and $R_{p_{STC}}$ calculated by the proposed method are utilised, the value of $V_{oc_{STC}}$ obtained from the proposed model becomes closest to the datasheet value. The accuracy of the model is maximum, when the values of a_{STC}, $R_{s_{STC}}$, and $R_{p_{STC}}$ calculated by the proposed technique are utilised for modeling.

(iv) A most generalized PV module model is build with MATLAB/Simulink by using the values of parameters of the *I-V* equation obtained from programming results in order to show the practical use of the proposed model.

(v) The proposed method proves to be more accurate in modeling commercially available PV modules as compared to other methods available in literature.

12. Future Work

Under partial shading condition (PSC) on a PV array, the irradiance and temperature of the PV modules undergoing shading change. The parameters of the shaded and unshaded PV modules of the array can be easily evaluated by employing the proposed method. By applying a suitable maximum power point tracking (MPPT) technique, maximum power point (MPP) of a PV array under PSC can be reached and hence MPPT can be ensured which will be the subject of our further investigations.

Nomenclature

$I_{\mathrm{pv,cell}}$: Photovoltaic current of the ideal PV cell (A)
$I_{0,\mathrm{cell}}$: Reverse saturation or leakage current of the ideal PV cell (A)
I_{pv}: Photovoltaic current of the PV module (A)
I_0: Reverse saturation or leakage current of the PV module (A)
a: Diode ideality constant of the PV module
R_{s}: Equivalent series resistance of the PV module (Ω)
R_{p}: Equivalent parallel resistance of the PV module (Ω)
V_{t}: Thermal voltage of the PV module (V)
q: Electron charge ($1.60217646 * 10^{-19}$C)
k: Boltzmann constant ($1.3806503 * 10^{-23}$ J/K)
G: Irradiance (W/m^2)
T: Temperature of the PV module (K)
N_{s}: Number of cells connected in series in the PV module
N_{p}: Number of parallel connections of cells in the PV module
P_{mpp}: Power of the PV module at the maximum power point (W)
V_{mpp}: Voltage of the PV module at the maximum power point (V)
I_{mpp}: Current of the PV module at the maximum power point (A)
V_{oc}: Open-circuit voltage of the PV module (V)
I_{sc}: Short-circuit current of the PV module (A)
$K^G_{P_{\mathrm{mpp}}}$: Irradiance coefficient of P_{mpp}
$K^T_{P_{\mathrm{mpp}}}$: Temperature coefficient of P_{mpp} (W/K)
$K^G_{V_{\mathrm{mpp}}}$: Irradiance coefficient of V_{mpp}
$K^T_{V_{\mathrm{mpp}}}$: Temperature coefficient of V_{mpp} (V/K)
$K^T_{I_{\mathrm{mpp}}}$: Temperature coefficient of I_{mpp} (A/K)
$K^G_{V_{\mathrm{oc}}}$: Irradiance coefficient of V_{oc}
$K^T_{V_{\mathrm{oc}}}$: Temperature coefficient of V_{oc} (V/K)
$K^T_{I_{\mathrm{sc}}}$: Temperature coefficient of I_{sc} (A/K).

Index

STC: Subscripts indicate the parameters at Standard Test Condition
NOCTC: Subscripts indicate the parameters at Nominal Operating Cell Temperature Condition.

Conflicts of Interest

The authors declare that there is no conflict of interest regarding the publication of this paper.

Acknowledgments

The authors wish to thank the Electrical Engineering Department of the National Institute of Technology Patna (India) for providing all the experimental facilities to carry out this work.

References

[1] S. A. Rahman, R. Varma, and T. Vanderheide, "Generalised model of a photovoltaic panel," *IET Renewable Power Generation*, vol. 8, no. 3, pp. 217–229, 2014.

[2] P. H. Huang, W. Xiao, J. C. H. Peng, and J. L. Kirtley, "Comprehensive parameterization of solar cell: improved accuracy with simulation efficiency," *IEEE Transactions on Industrial Electronics*, vol. 63, pp. 1549–1560, 2016.

[3] X. Feng, X. Qing, C. Y. Chung, H. Qiao, X. Wang, and X. Zhao, "A simple parameter estimation approach to modeling of photovoltaic modules based on datasheet values," *Journal of Solar Energy Engineering*, vol. 138, no. 5, article 0510108, 2016.

[4] M. G. Villalva, J. R. Gazoli, and E. R. Filho, "Comprehensive approach to modeling and simulation of photovoltaic arrays," *IEEE Transactions on Power Electronics*, vol. 24, no. 5, pp. 1198–1208, 2009.

[5] W. De Soto, S. A. Klein, and W. A. Beckman, "Improvement and validation of a model for photovoltaic array performance," *Solar Energy*, vol. 80, no. 1, pp. 78–88, 2006.

[6] G. R. Walker, "Evaluating MPPT converter topologies using a MATLAB PV model," *Journal of Electrical and Electronics Engineering*, vol. 21, no. 1, pp. 49–55, 2001.

[7] H. N. Mohamed and S. A. Mahmoud, "Temperature dependence in modeling photovoltaic arrays," in *2013 IEEE 20th International Conference on Electronics, Circuits, and Systems (ICECS)*, pp. 747–750, Abu Dhabi, United Arab Emirates, 2013.

[8] V. J. Chin, Z. Salam, and K. Ishaque, "An accurate modelling of the two-diode model of PV module using a hybrid solution based on differential evolution," *Energy Conversion and Management*, vol. 124, p. 4250, 2016.

[9] B. C. Babu and S. Gurjar, "A novel simplified two-diode model of photovoltaic (PV) module," *IEEE Journal of Photovoltaics*, vol. 4, pp. 1156–1161, 2014.

[10] D. H. Muhsen, A. B. Ghazali, T. Khatib, and I. A. Abed, "Parameters extraction of double diode photovoltaic module's model based on hybrid evolutionary algorithm," *Energy Conversion and Management*, vol. 105, pp. 552–561, 2015.

[11] J. A. Gow and C. D. Manning, “Development of a photovoltaic array model for use in power-electronics simulation studies,” *IEE Proceedings - Electric Power Applications*, vol. 146, no. 2, pp. 193–200, 1999.

[12] K. Ishaque, Z. Salam, and H. Taheri, “Simple, fast and accurate two-diode model for photovoltaic modules,” *Solar Energy Materials and Solar Cells*, vol. 95, no. 2, pp. 586–594, 2011.

[13] S. Lun, S. Wang, T. Guo, and C. Du, “An *I–V* model based on time warp invariant echo state network for photovoltaic array with shaded solar cells,” *Solar Energy*, vol. 105, pp. 529–541, 2014.

[14] A. Oi, *Design and simulation of photovoltaic water pumping system, [M.S. thesis]*, Faculty of California Polytechnic State University, San Luis Obispo, CA, USA, 2005.

[15] MATLAB demos, “Solar cell parameter extraction from data,” November 2017, http://in.mathworks.com/help/physmod/elec/examples/solar-cell-parameter-extraction-from-data.html.

[16] “Solar panels, 5th Generation a-Si solar panels, Datasheet,” November 2017, http://www.apexpowerconcepts.com/fee-20-12.pdf.

[17] A. N. Celik and N. Acikgoz, “Modelling and experimental verification of the operating current of mono-crystalline photovoltaic modules using four- and five-parameter models,” *Applied Energy*, vol. 84, no. 1, pp. 1–15, 2007.

[18] I. H. Altas and A. M. Sharaf, “A photovoltaic array simulation model for Matlab-Simulink GUI environment,” in *2007 International Conference on Clean Electrical Power*, pp. 341–345, Capri, Itlay, 2007.

[19] N. N. B. Ulapane, C. H. Dhanapala, S. M. Wickramasinghe, S. G. Abeyratne, N. Rathnayake, and P. J. Binduhewa, “Extraction of parameters for simulating photovoltaic panels,” in *2011 6th International Conference on Industrial and Information Systems*, Kandy, Sri Lanka, August 2011.

[20] M. C. Glass, “Improved solar array power point model with SPICE realization,” in *IECEC 96. Proceedings of the 31st Intersociety Energy Conversion Engineering Conference*, pp. 286–291, Washington, DC, USA, August 1996.

[21] Y. T. Tan, D. S. Kirschen, and N. Jenkins, “A model of PV generation suitable for stability analysis,” *IEEE Transactions on Energy Conversion*, vol. 19, no. 4, pp. 748–755, 2004.

[22] T. Aernouts, W. Geens, J. Poortmans, P. Heremans, S. Borghs, and R. Mertens, “Extraction of bulk and contact components of the series resistance in organic bulk donor-acceptor-heterojunctions,” *Thin Solid Films*, vol. 403-404, pp. 297–301, 2002.

[23] D. S. H. Chan and J. C. H. Phang, “Analytical methods for the extraction of solar-cell single- and double-diode model parameters from I-V characteristics,” *IEEE Transactions on Electron Devices*, vol. 34, no. 2, pp. 286–293, 1987.

[24] S.-x. Lun, S. Wang, G.-h. Yang, and T.-t. Guo, “A new explicit double-diode modeling method based on Lambert W-function for photovoltaic arrays,” *Solar Energy*, vol. 116, pp. 69–82, 2015.

[25] T. F. Elshatter, M. T. Elhagree, M. E. Aboueldahab, and A. A. Elkousry, “Fuzzy modeling and simulation of photovoltaic system,” in *Proceedings of the 14th European Photovoltaic Solar Energy Conference*, 1997.

[26] A. Mellit, M. Benghanem, and S. A. Kalogirou, “Modeling and simulation of a stand-alone photovoltaic system using an adaptive artificial neural network: proposition for a new sizing procedure,” *Renewable Energy*, vol. 32, pp. 285–313, 2007.

[27] F. Almonacid, C. Rus, L. Hontoria, and F. J. Munoz, “Characterisation of PV CIS module by artificial neural networks. A comparative study with other methods,” *Renewable Energy*, vol. 35, pp. 973–980, 2010.

[28] S. Jing Jun and L. Kay-Soon, “Photovoltaic model identification using particle swarm optimization with inverse barrier constraint,” *IEEE Transactions on Power Electronics*, vol. 27, no. 9, pp. 3975–3983, 2012.

[29] R. C. Campbell, “A circuit-based photovoltaic array model for power system studies,” July 2010, http://www.ee.washington.edu/research/sesame/publication/Conference/2007/Campbell_PWL_PV_Model_NAPS2007.pdf.

[30] “Shell solar product information sheet,” http://www.atlantasolar.com/pdf/Shell/ShellST40_USv1.pdf.

[31] “First solar FS-270 (70W) solar panel,” September 2017, http://www.firstsolar.com/en-IN/-/media/First-Solar/Technical-Documents/Series-2-Datasheets/Series-2-Module-Datasheet-NA.ashx?la=en.

[32] “Shell solar product information sheet,” http://www.physics.arizona.edu/~cronin/Solar/TEP%20module%20spec%20sheets/Shell%20SQ150.pdf.

[33] “HIT photovoltaic module, HIT-N240SE10 HIT-N235SE10 HIT N230SE10 datasheet,” 2017, http://future-energy-solutions.co.uk/wp-content/uploads/2014/10/Panasonic-Datasheet-HIT-240W.pdf.

[34] “KD140GX-LFBS, KD 135 F series - Kyocera Solar datasheet,” http://www.kyocerasolar.com/dealers/product-center/.

[35] “KD260GX-LFB2, KD 200-60F series - Kyocera Solar datasheet,” http://www.kyocerasolar.com/dealers/product-center/.

[36] “KU265-6MCA, KU 200-60F series - Kyocera Solar atasheet,” http://www.kyocerasolar.com/dealers/product-center/.